



A Flow-Driven Cavity as an Air Cycling Model for Window Flow

Justin Campbell

Amanda Hiett

Akhil Sadam

Abstract

A lid-driven cavity is flow-driven to describe stress on and circulation inside buildings and small insect-to-UAV-size aircraft due to open windows or sidewall punctures. The transition between steady & unsteady flow is also roughly bounded, by investigating the Reynolds number at 4 values between 10 to 10^4 . A sparse simulation of low-speed and much higher-speed incompressible flows is undertaken, estimating feature shapes at the minimum computational cost.

Keywords: computational fluid dynamics, CFD, incompressible, Paraview, R, Python, coe347, spring 2022, window, building, tornado, high, reynolds, unsteady, steady, stress, strain, rate, mixing, volumetric, flow.

1. Motivation

For severe storms, it is widely known that puncture damage is the primary cause of failure for most buildings and aircraft. Once a puncture has been created, the resultant pressure differential can cause fast inflow and damage to the interior. We seek to study this inflow, and stresses near the opening walls, which can cause structural issues leading to collapse of one or more walls.

Most relevant studies use incredibly large amounts of computational power, due to the large scale of the problem (Reynolds numbers for tornadoes and hurricanes can easily start in the millions). We seek to show the applicability of lower Reynolds simulations to higher Reynolds situations, since the general large-scale flow structure remains the same.

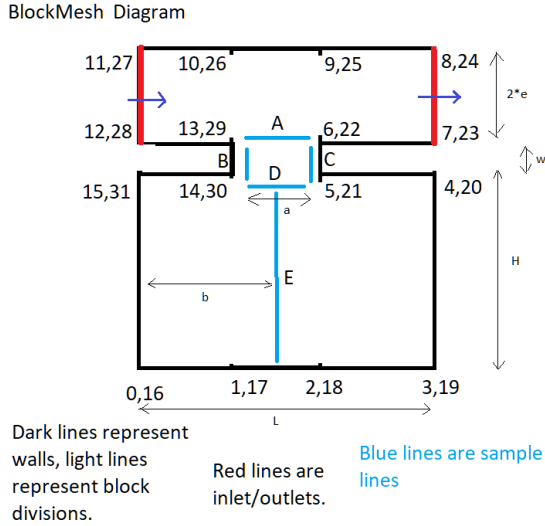
2. Implementation

We implement all simulation with OpenFoam, analysis with Paraview and Python3, and documentation code in R [Xie, Dervieux, and Riederer \(2020\)](#).

3. Mesh Assembly

We assemble a 2D mesh template as below, with the following parameters, all lengths nondimensionalized in terms of dimension L :

mutable: wall thickness w , window width a ,
 immutable: window location $b = 0.5$, cavity height $H = 1$, cavity width $L = 1$, and free-stream width $2e = 0.1$.



Two sets of simulations are performed, one for the low Reynolds (Re) numbers of 10 and 200, which will be shown to be steady, and another for $Re = 1000, 10000$.

Each mesh also has a corresponding refinement, which is described by the *meshFactor* parameter, representing the refinement in each dimension.

Full lists are available below.

3.1. Meshes for the Low Reynolds simulations

meshfactor	Reynolds	a	w
5	10	0.05	0.05
5	10	0.05	0.10
5	10	0.50	0.05
5	10	0.50	0.10
10	10	0.05	0.05
10	10	0.05	0.10
10	10	0.50	0.05
10	10	0.50	0.10
5	200	0.05	0.05
5	200	0.05	0.10
5	200	0.50	0.05
5	200	0.50	0.10
10	200	0.05	0.05
10	200	0.05	0.10
10	200	0.50	0.05
10	200	0.50	0.10

Table 1:

3.2. Meshes for the High Reynolds simulations

meshfactor	Reynolds	a	w
3	1000	0.5	0.1
5	1000	0.5	0.1
3	10000	0.5	0.1
5	10000	0.5	0.1

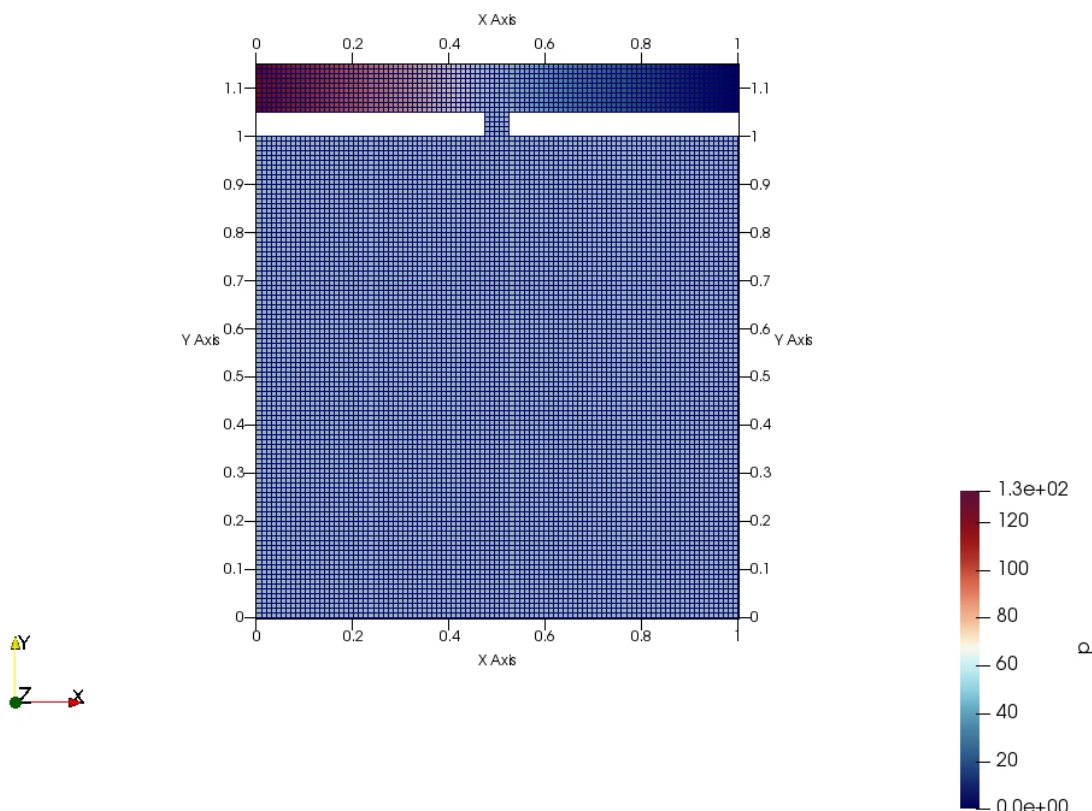
Table 2:

BlockMeshDict and similar files are available at [the repository](#).

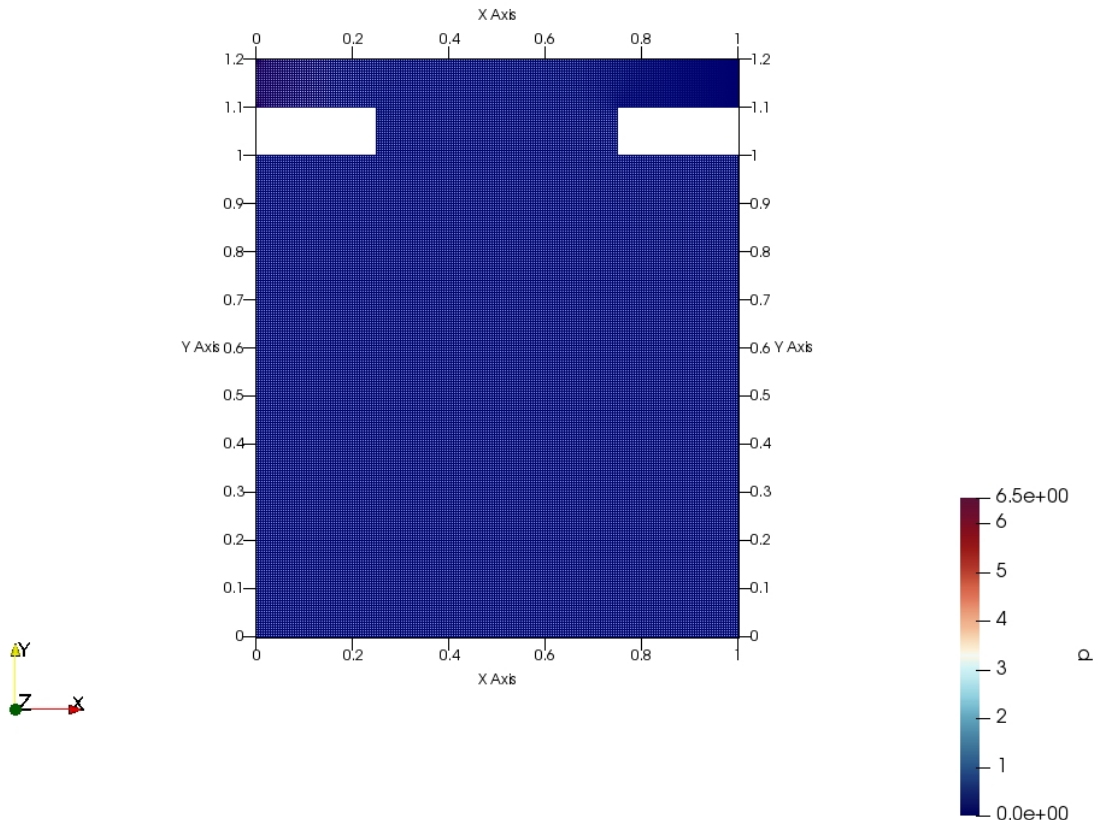
3.3. Mesh Images

A couple mesh samples are shown here; see the appendix for all images.

meshFactor, Re, windowWidth, wallThickness=5, 10, 0.05, 0.05:



meshFactor, Re, windowWidth, wallThickness=10, 200, 0.5, 0.1:



Now that the mesh resolutions can be seen as adequate, we will move to results.

4. Literature Review

Wind speeds may be categorized as dangerous once reaching the threshold of 50mph. Winds of this caliber may occur during storms and tornados, and can be catastrophic to infrastructure.(2019; Hadhazy 2011; Tessner 2021)

Structurally, windows are weak in comparison to the surrounding structure and therefore are generally the first to break when confronted with strong winds. The missing window then creates a cavity with a pressure differential to the outside wind that may encourage further destruction. The fragility of windows is why many coastal buildings near hurricane hotspots have shutters, and in the event of a storm, those without shutters often cover their windows with materials such as plywood to protect against the oncoming winds.(2019; Hadhazy 2011; Tessner 2021)

The average home is designed to withstand winds of 90mph for around 3 seconds, which is far from sufficient to withstand even a moderate class of tornado. Especially when including forces working in tandem generating lift on top of normal stressors. As roof connections rely primarily on gravity to ensure stability, any opposing force to gravity need only overcome the weight force of the roof to remove it from the structure entirely.(2019; Hadhazy 2011; Tessner 2021)

Due to the propensity of air to create vortices when exposed to nonzero velocity and pressure differential, the way air may travel through the structure could pose an additional destructor on top of the exterior conditions. It has been proven advantageous for homes in storm-prone areas to install shutters, so prevention of inducing cavity-like flow on a structure is of import.(2019; Hadhazy 2011; Tessner 2021)

5. Low Reynolds Number

Note all values are nondimensionalized - all lengths are in terms of L , the cavity length, all speeds in terms of U , the initial flow speed, and all times in terms of $\frac{L}{U}$.

The pressure is in terms of $\frac{p}{\rho U^2}$. All low-Reynolds simulations were run till $T=6$.

5.4. General Solution Form

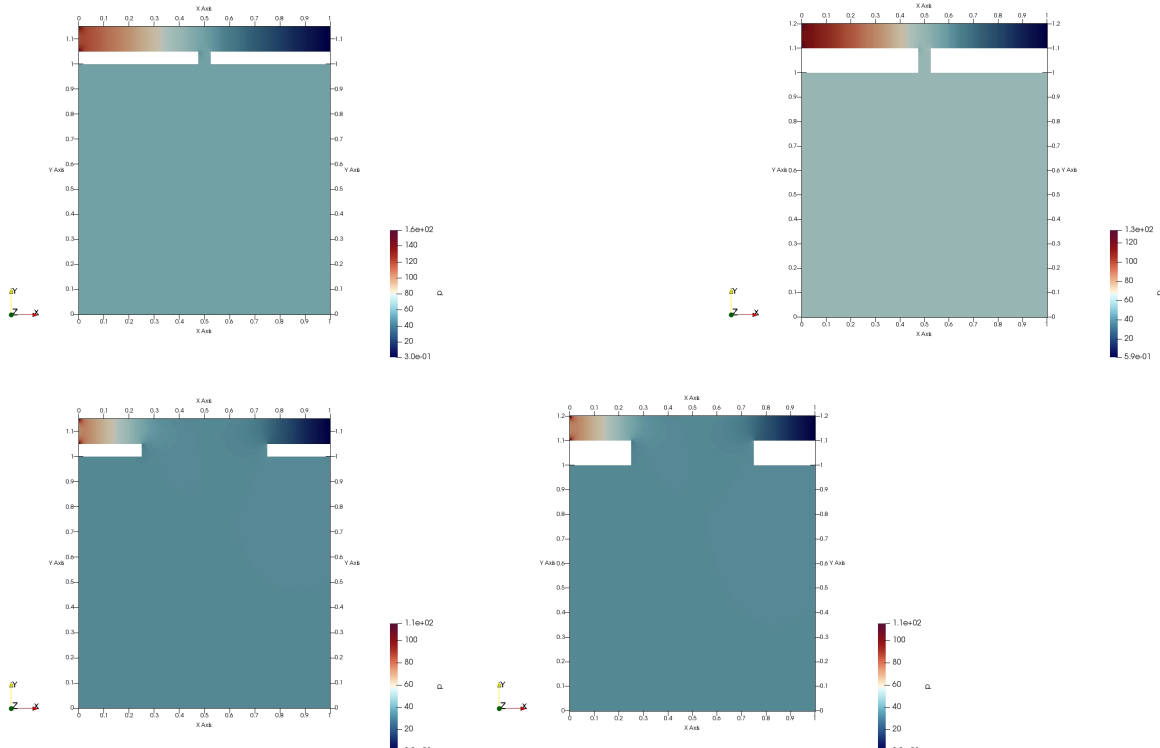
We will now show the pressure, X-velocity, Y-velocity, and streamlines in sets of 4 by varying geometry along the following pattern. Contours are not shown due to their bias toward out-of-cavity portions and the coarse mesh will be omitted for brevity. Convergence studies will be done numerically afterward.

Pattern:

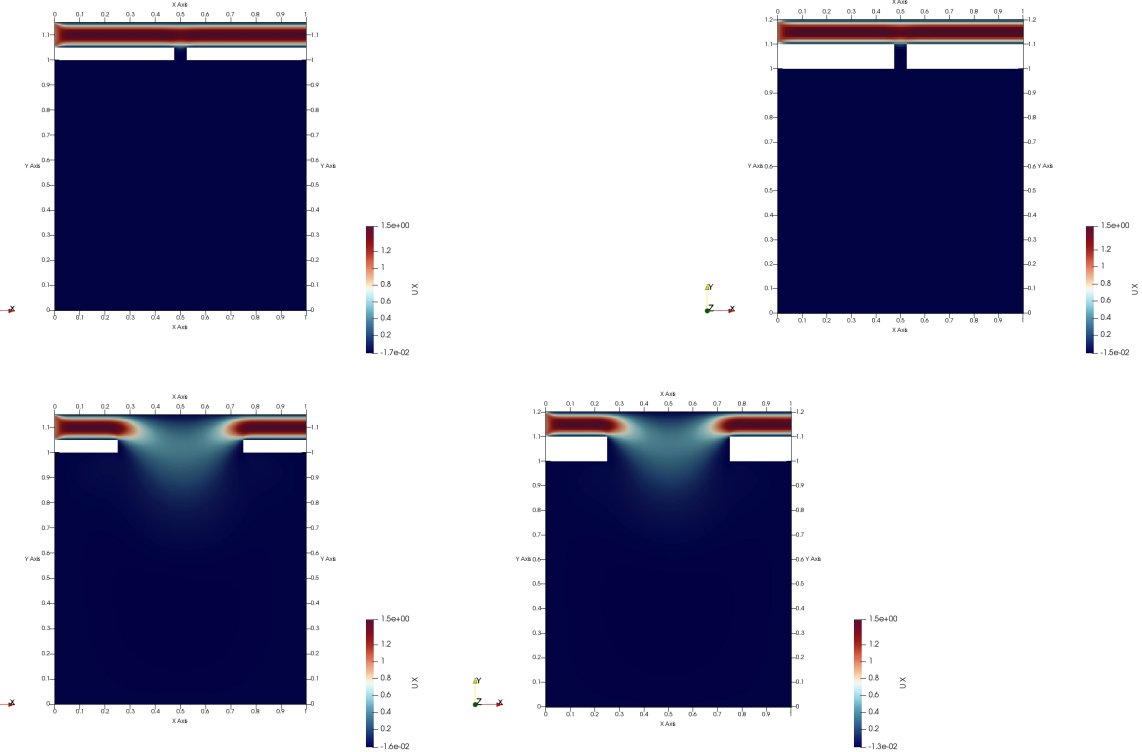
window.size.a	wall.thickness.w
0.05	0.05
0.05	0.10
0.50	0.05
0.50	0.10

Table 3:

Re=10, Pressure

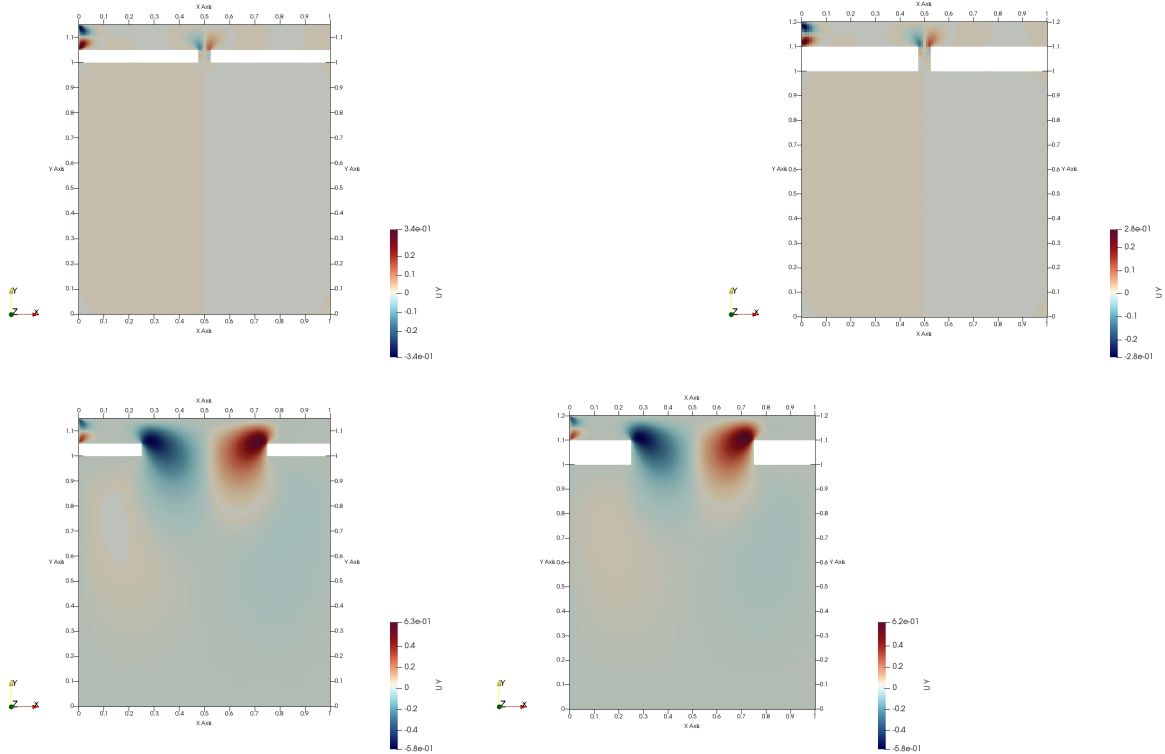


Note that all meshes have relatively even internal pressure, suggesting internal flow speeds are minuscule. Also, the more contact the cavity has with the crossflow, the lower the internal cavity pressure. Finally, consider the inlet. Note that the higher-pressure regions localize at the corners with larger windows, implying that the cavity acts as a sort of pressure sink.

Re=10, X-velocity

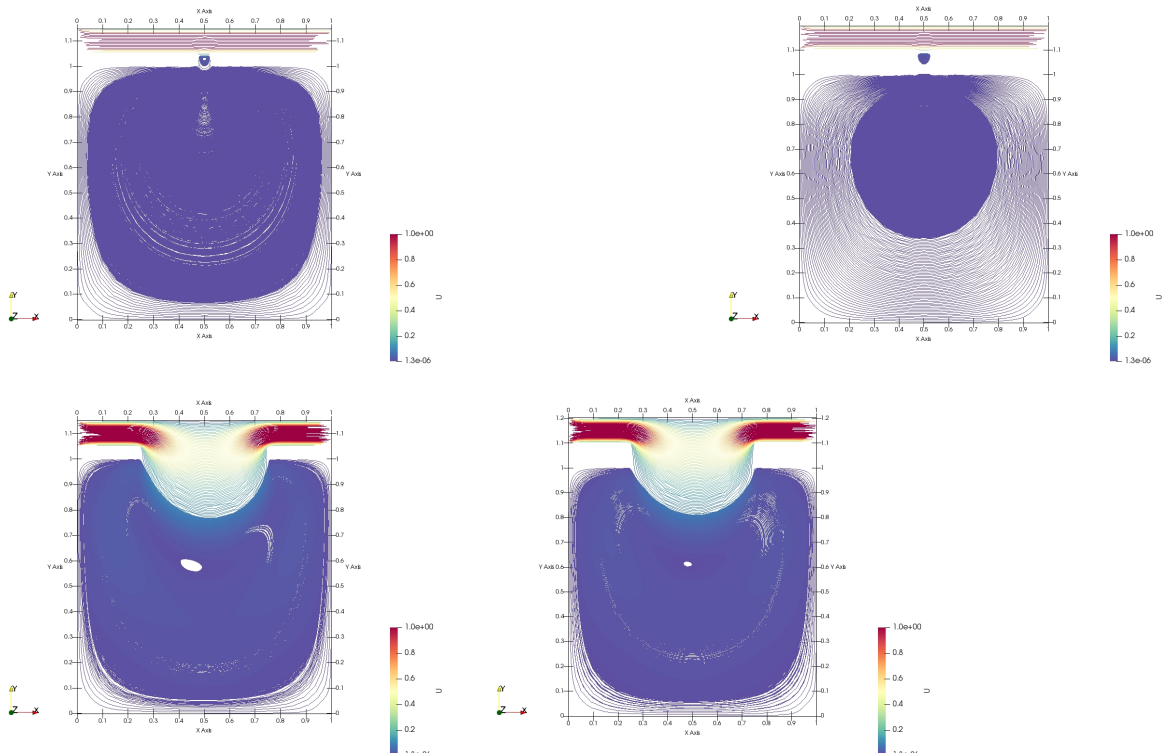
Similarly, the flow x-velocity dissipates across the window in amounts positively correlated with larger and thinner windows. No discernible cavity flow can be seen yet.

Re=10, Y-velocity



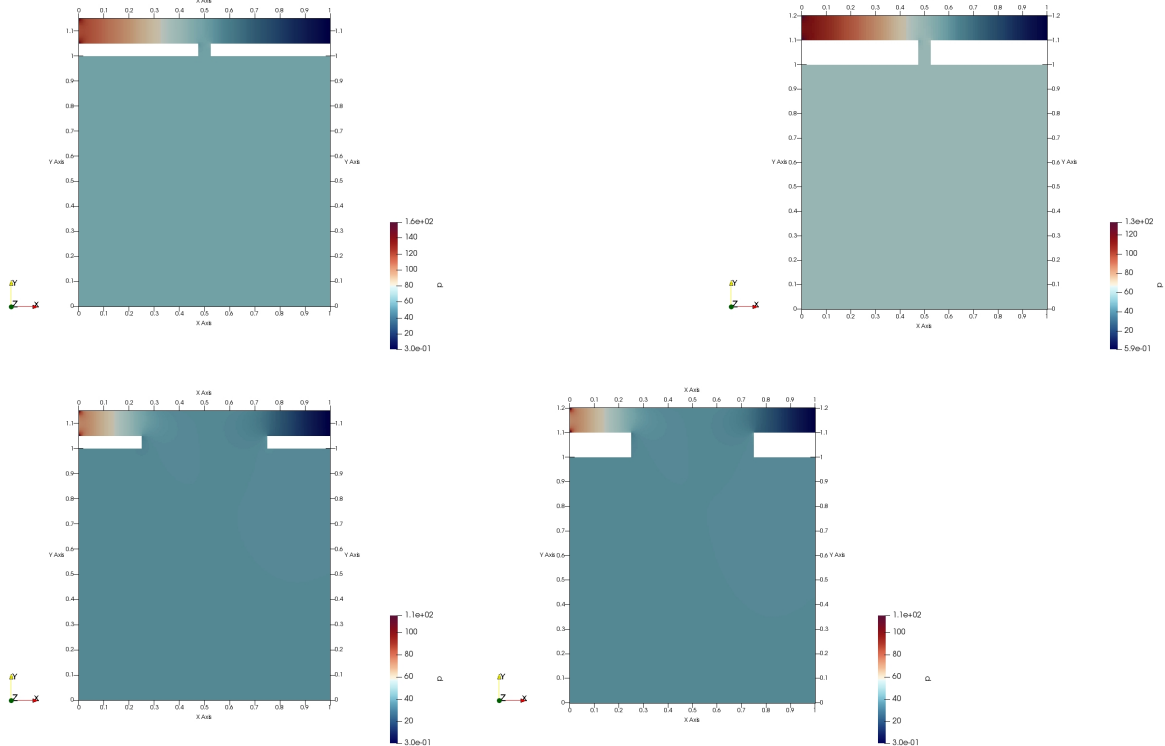
The same story can be seen in the y-velocities, but now there can be seen a cavity circulation (by the mild color differences inside the cavity). Note that the windows of 0.05 width produce really mild, near-complete cavity circulation, while the larger windows of 0.5 width produce much stronger but incomplete circulation (the corners are relatively unaffected).

Re=10, Streamlines



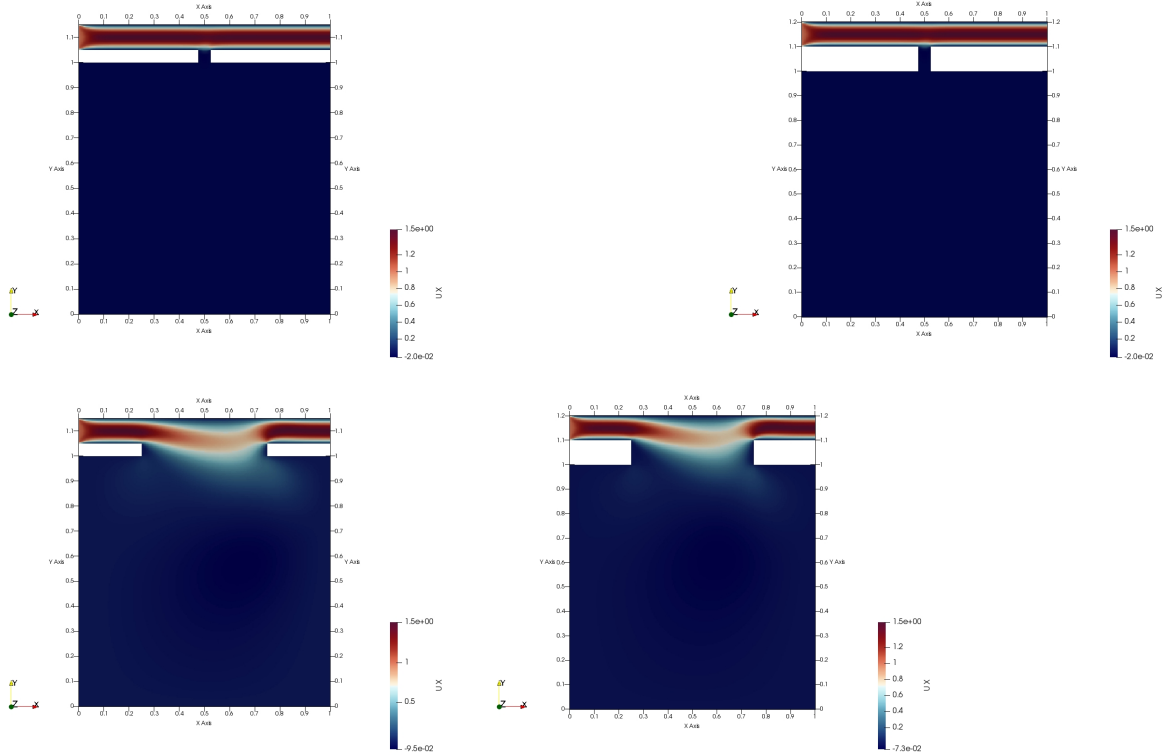
This is confirmed by the streamline plots. Note that there are between 1-3 transition vortices. At maximum, with the most neck-like window, there is a vortice the window opening, one in the window another in opening to the cavity. These three vortices connect the crossflow to the internal centralized vortex. When the window is broadened, these vortices all combine to form a single large transition vortice. Finally, note the center of the centralized vortice is very close to the center, and the crossflow bend is similarly symmetric, despite the flow directionality. This symmetry is probably due to the low Reynolds number of the flow.

Re=200, Pressure



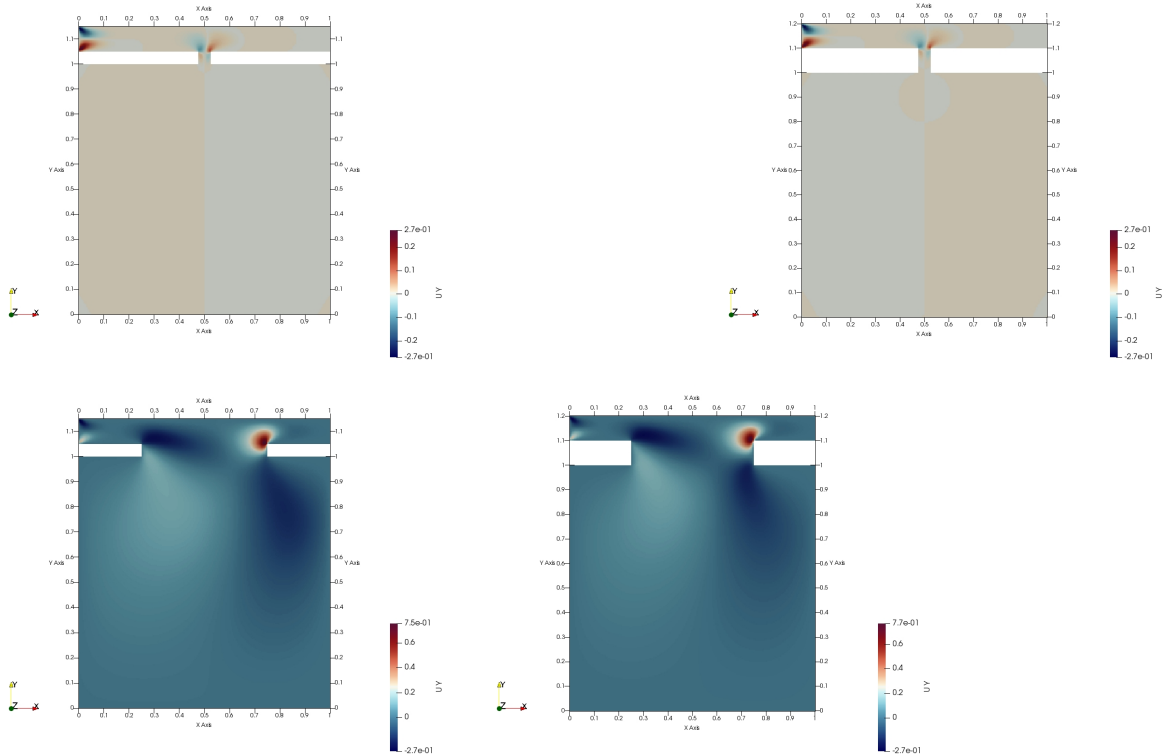
The pressure for Re=200 is very similar to that of Re=10 - the cavity acts like a simple pressure sink.

Re=200, X-velocity



The only major difference is the asymmetry, which is probably due to the Reynolds number. Note that these solutions are also stable, and have been checked by flow visualization over time.

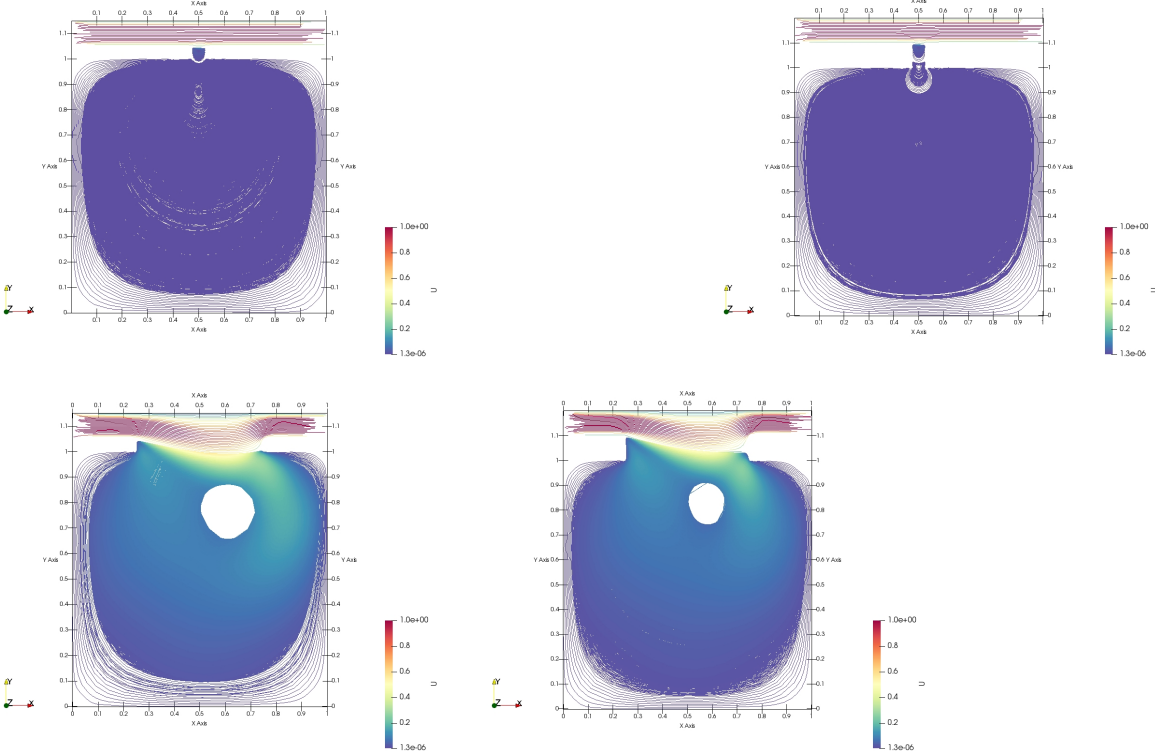
Re=200, Y-velocity



Note that in addition to the asymmetry (same as seen in the x-velocity plots), there is an additional hydraulic jump right at the upper-right window corner, as the flow resumes high speed.

We will return to this in the high Reynolds section, as with increasing Re, this sort of jump can cause additional effects. We can also see the prominent third transition vortice clearly in the top-right plot.

Re=200, Streamlines



Note the prominent third transition vortice. Otherwise, everything is as expected from Re=10 flow, except for the asymmetry.

5.5. Vortice Positions

Convergence can easily be seen by looking at the centralized vortex position for both meshes, by differing geometry.

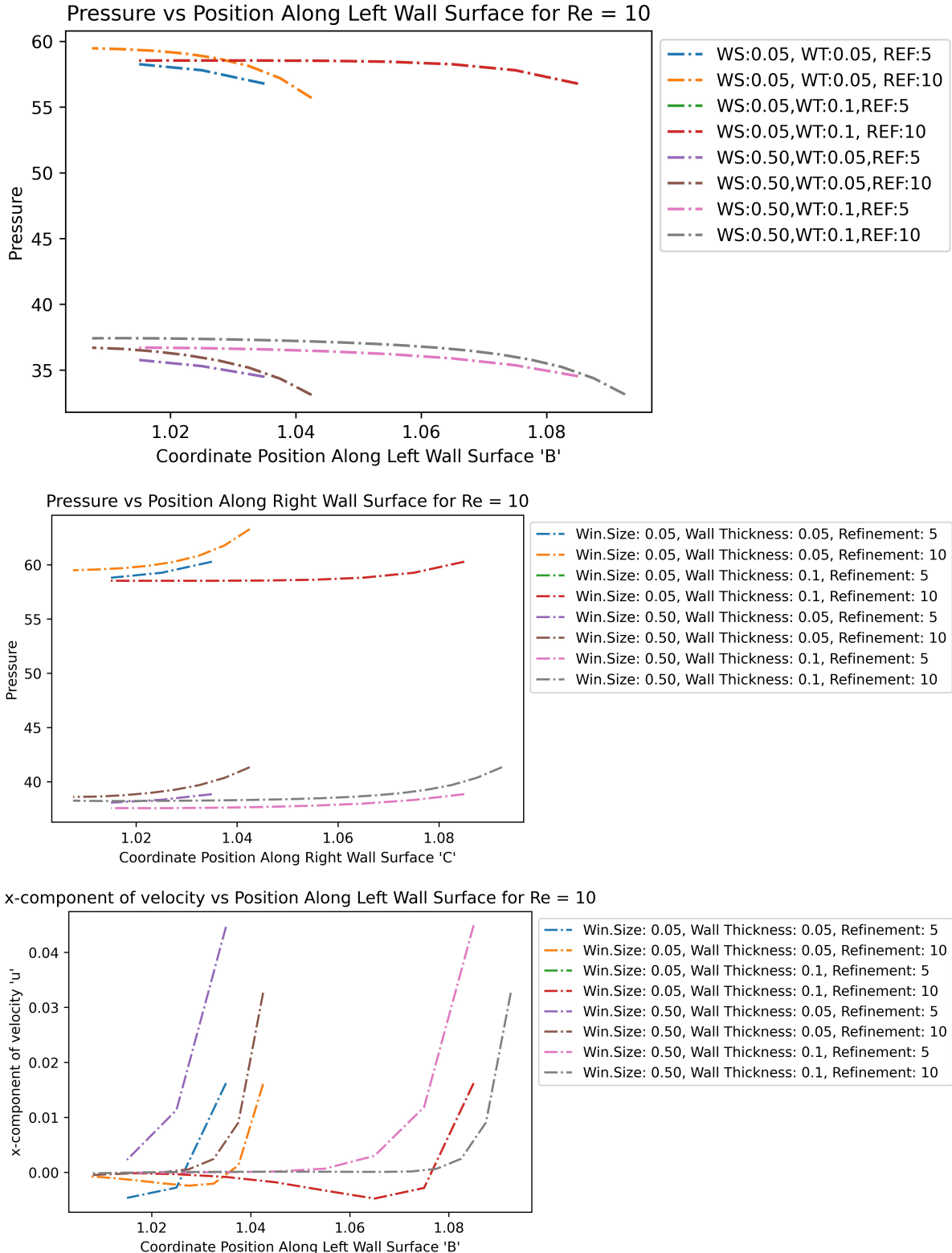
meshfactor	Reynolds	window.a.	wall.w.	Vortex.Center.Location.along.Y
5	10	0.05	0.05	0.8350
10	10	0.05	0.05	0.8525
5	10	0.05	0.10	0.9650
10	10	0.05	0.10	0.9650
5	10	0.50	0.05	0.5650
10	10	0.50	0.05	0.5725
5	10	0.50	0.10	0.6050
10	10	0.50	0.10	0.6075
5	50	0.05	0.05	0.8350
10	50	0.05	0.05	0.8525
5	50	0.05	0.10	0.9650
10	50	0.05	0.10	0.6075
5	50	0.50	0.05	0.6550
10	50	0.50	0.05	0.6625
5	50	0.50	0.10	0.6850
10	50	0.50	0.10	0.6875
5	200	0.05	0.05	0.8550
10	200	0.05	0.05	0.8675
5	200	0.05	0.10	0.9750
10	200	0.05	0.10	0.6875
5	200	0.50	0.05	0.7650
10	200	0.50	0.05	0.7725
5	200	0.50	0.10	0.8250
10	200	0.50	0.10	0.8325

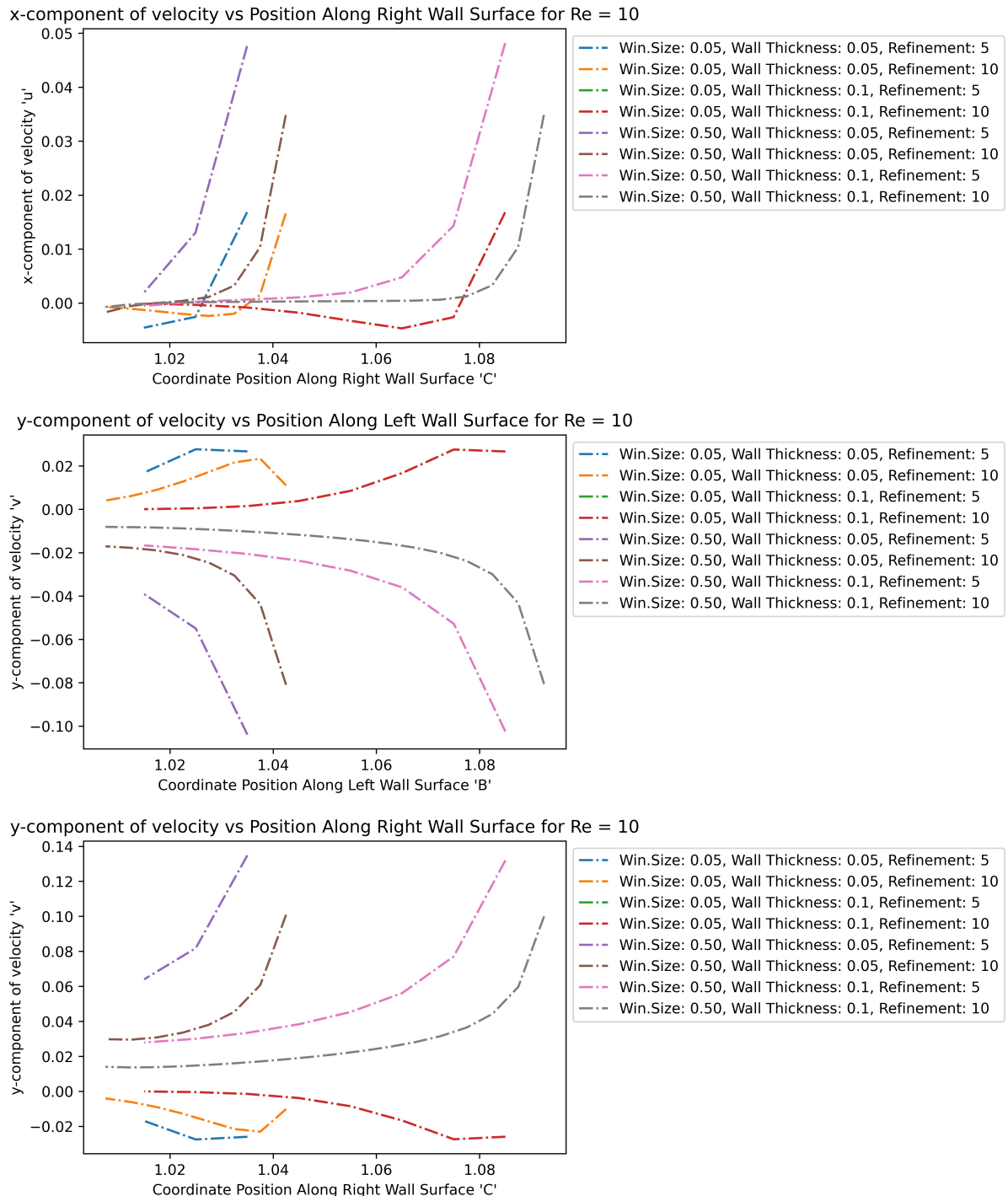
Table 4:

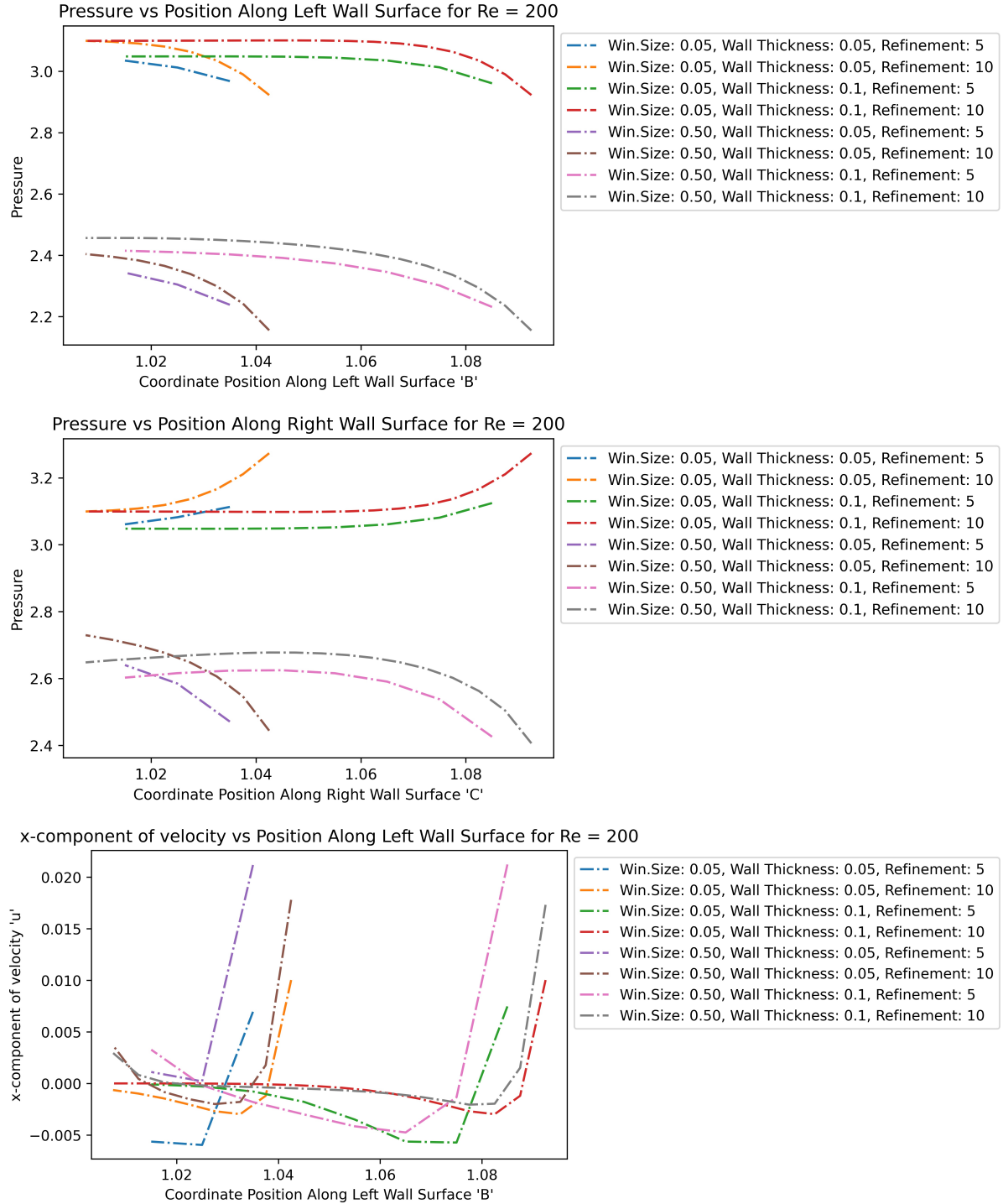
5.6. Window Wall Solution Profiles

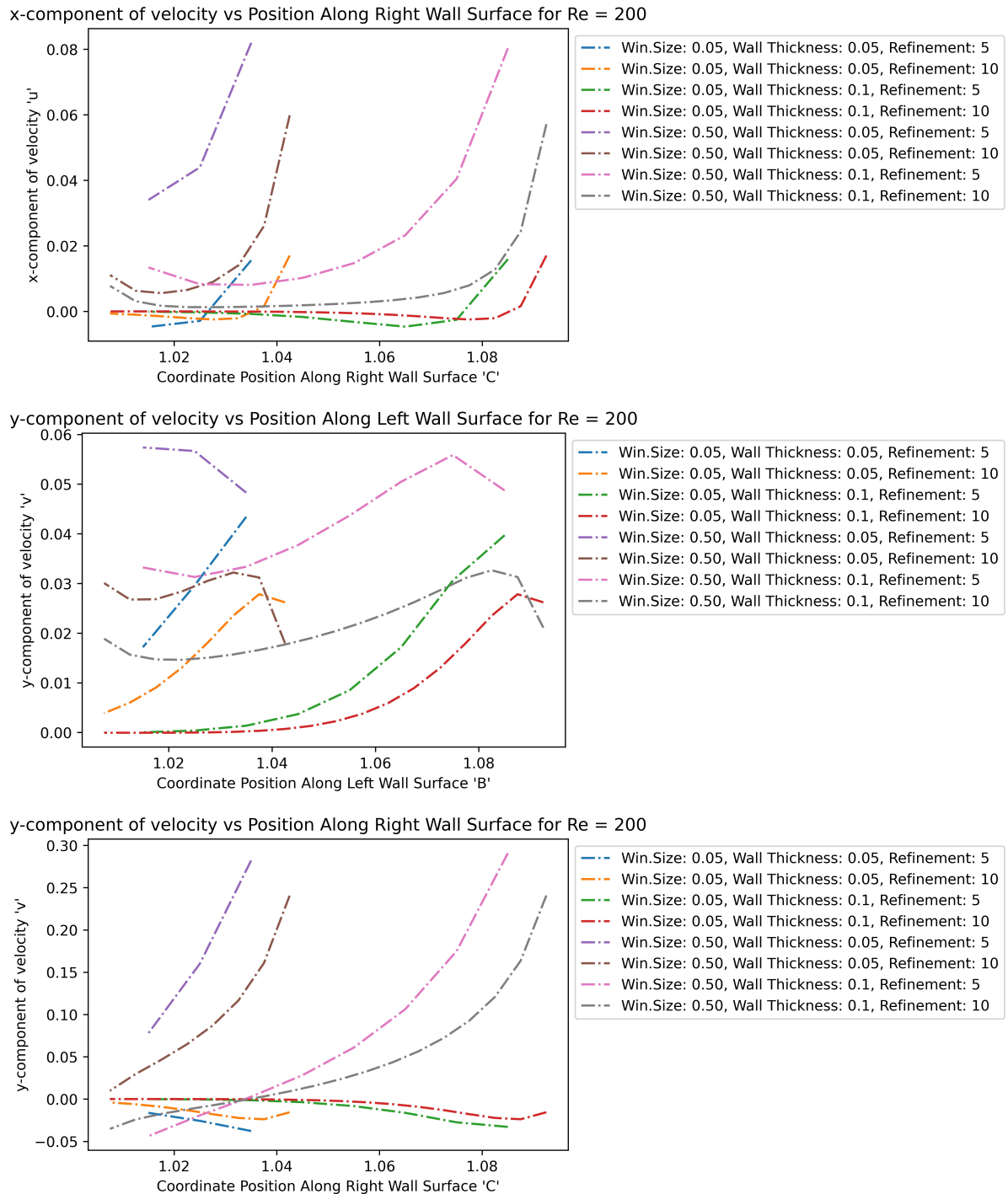
Now consider the profiles along the left and right window walls; the vertical segments along the inside of the window.

Re=10



**Re=200**

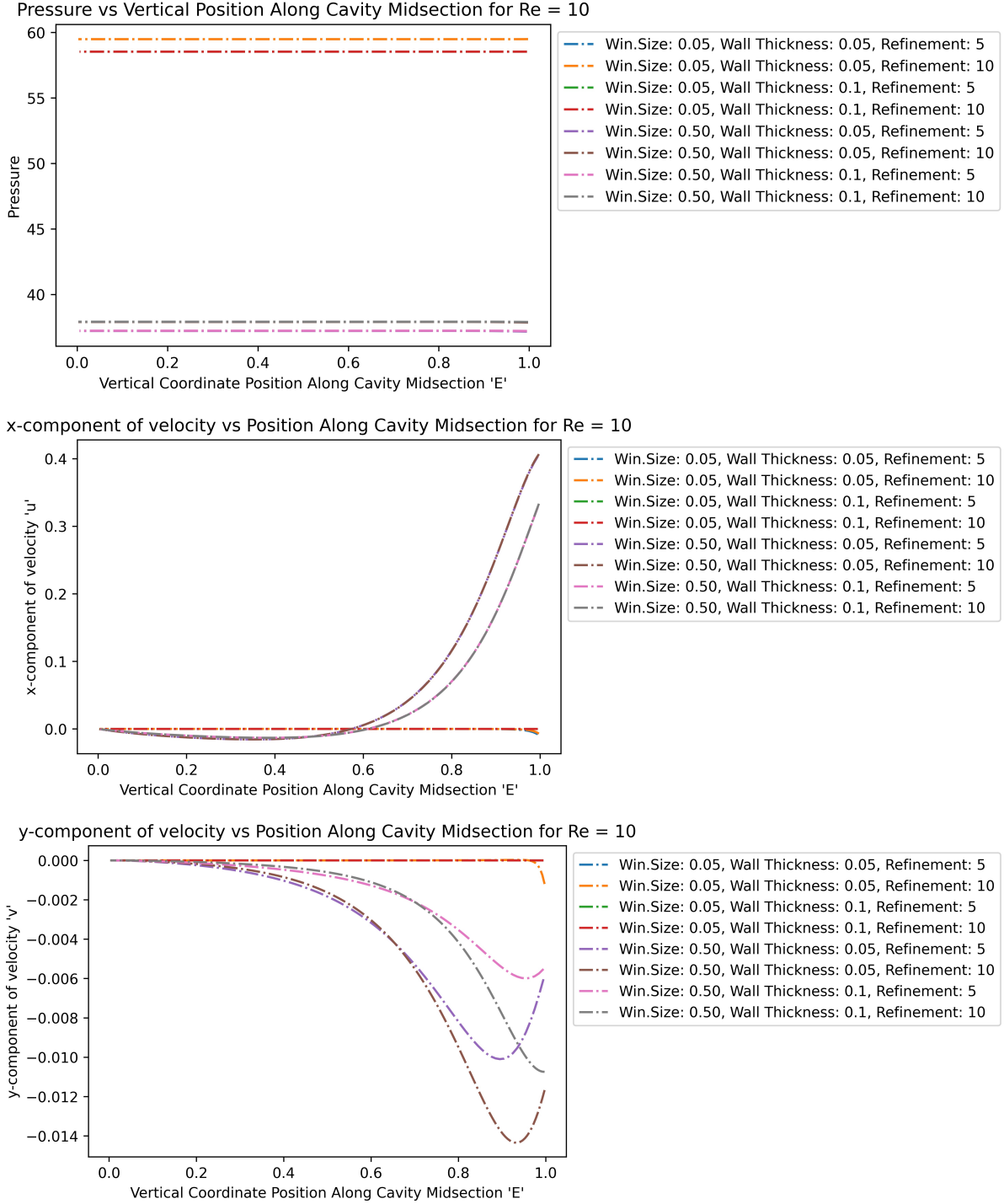




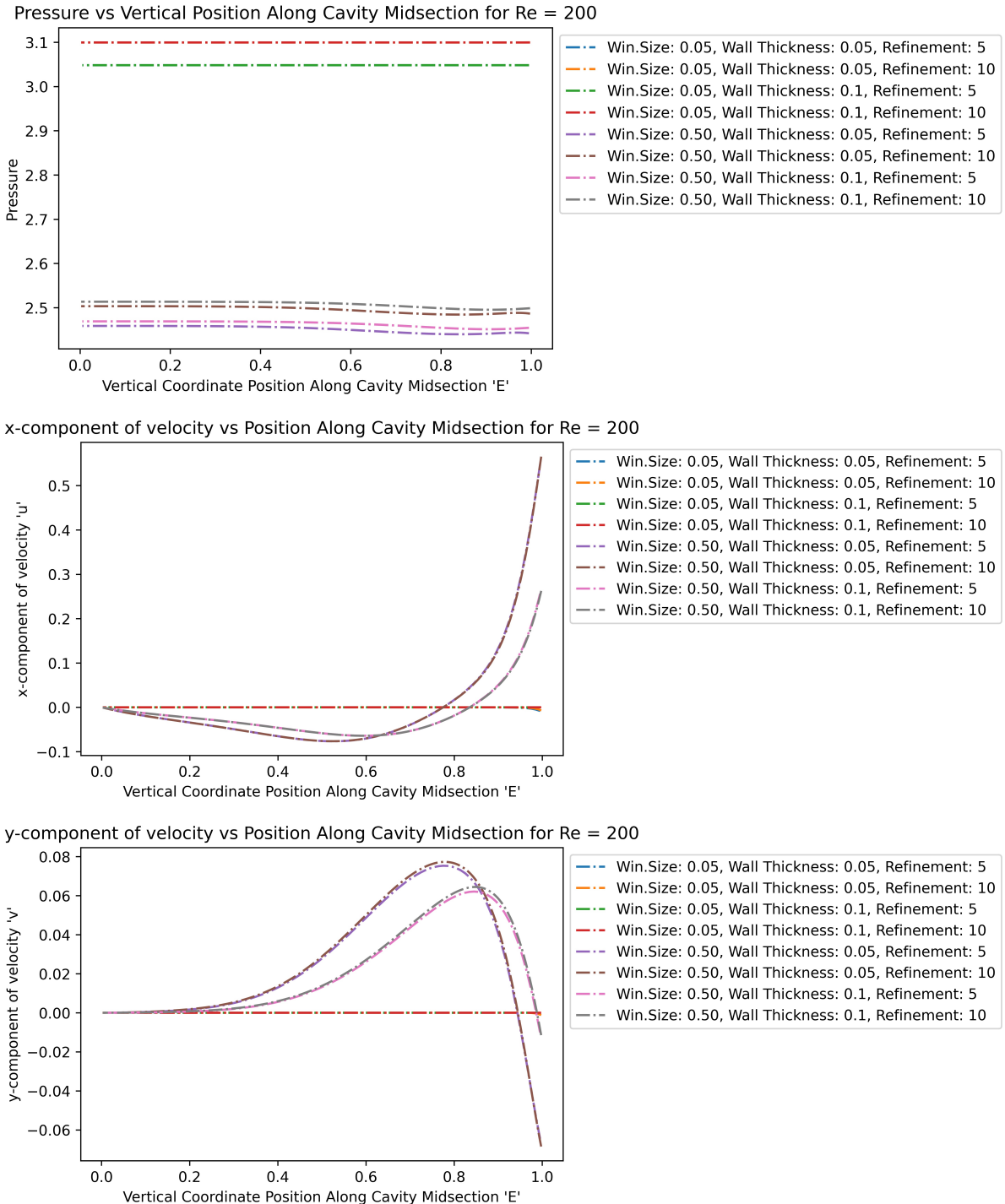
5.7. Cavity Midline Solution Profile

Now consider the profiles along the vertical midline down the cavity; from the middle of the window down to the back of the cavity.

Re=10



Re=200



6. High Reynolds Number Part 1

Note again all values are nondimensionalized - all lengths are in terms of L , the cavity length, all speeds in terms of U , the initial flow speed, and all times in terms of $\frac{L}{U}$.

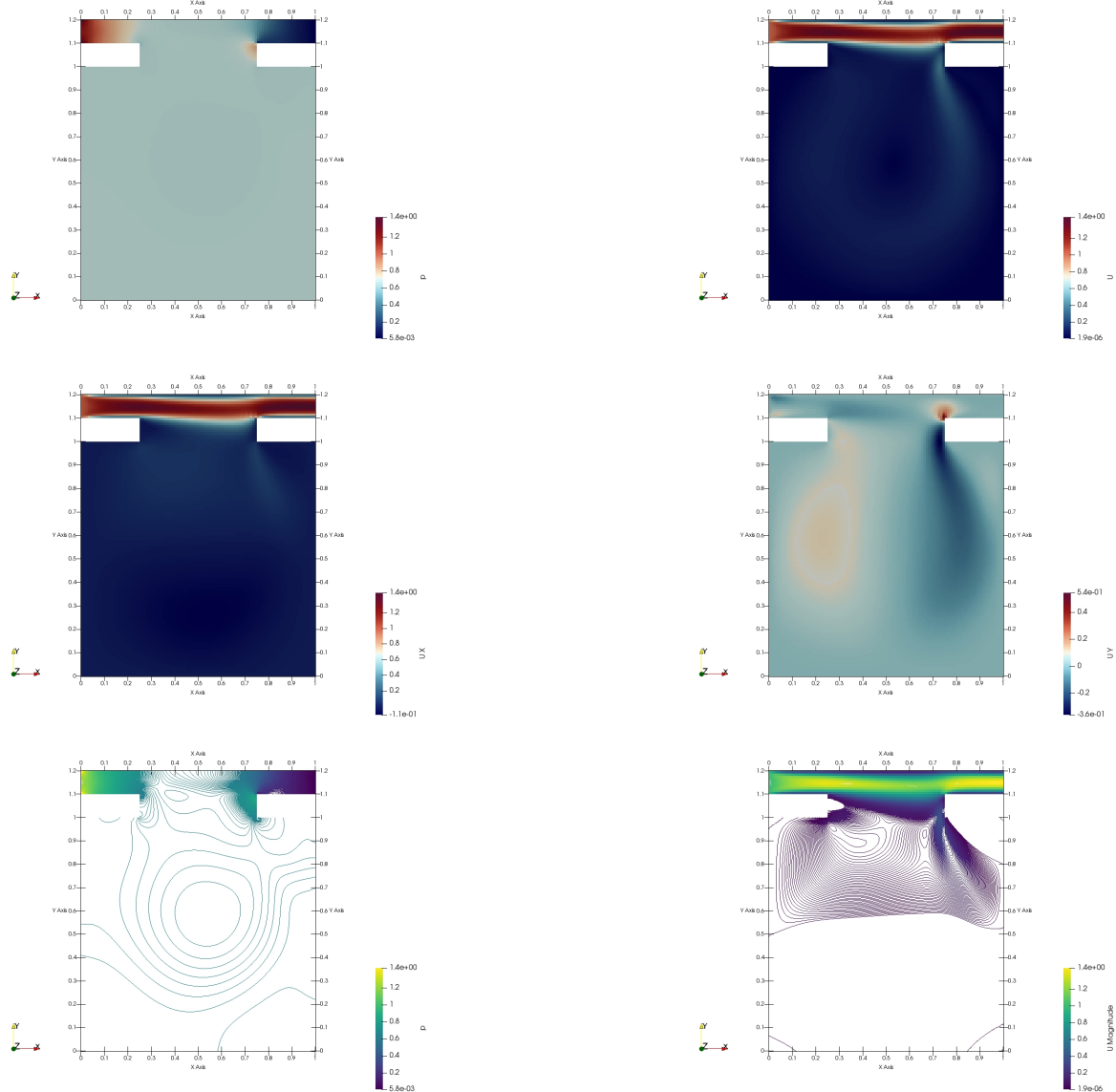
The pressure is in terms of $\frac{p}{\rho U^2}$.

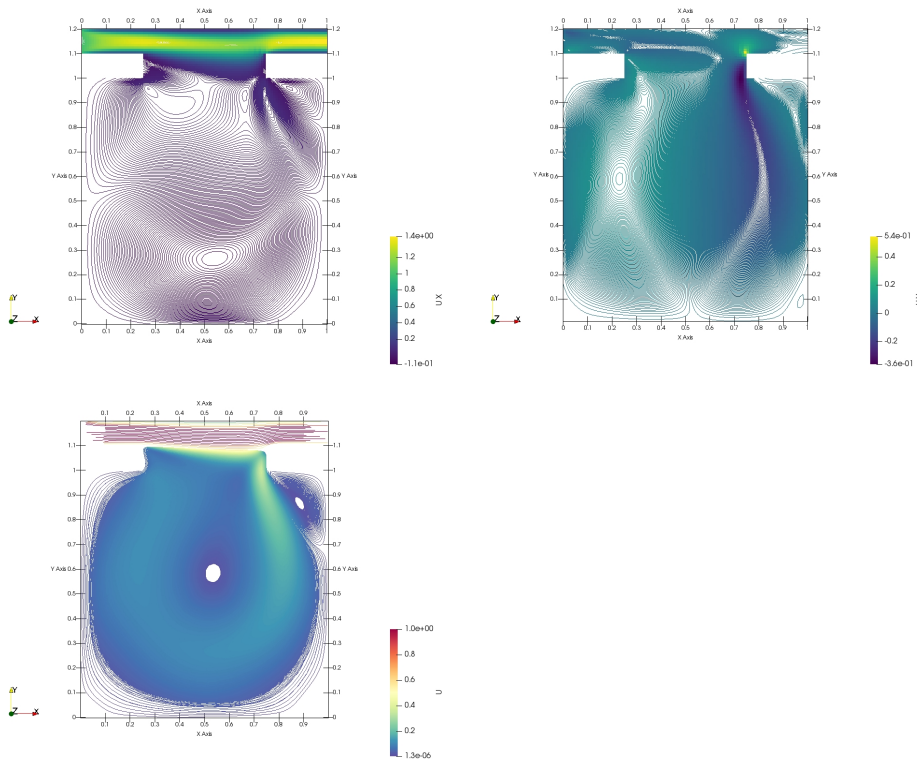
6.8. General Solution Form

Given the results from the Low Reynolds simulations, we will now consider only a window width of 0.5 and a wall thickness of 0.1. Images only for the refined mesh will be shown, for brevity.

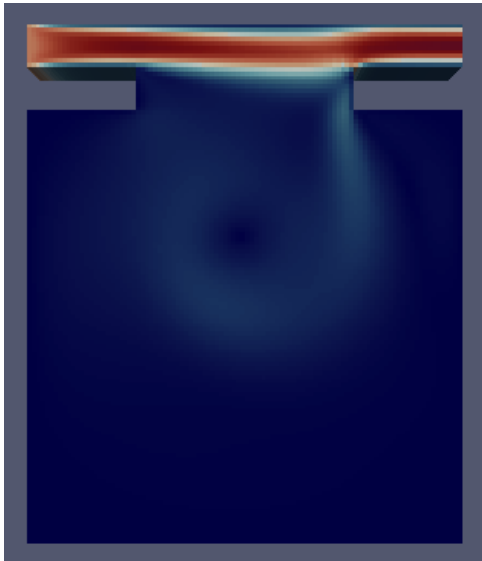
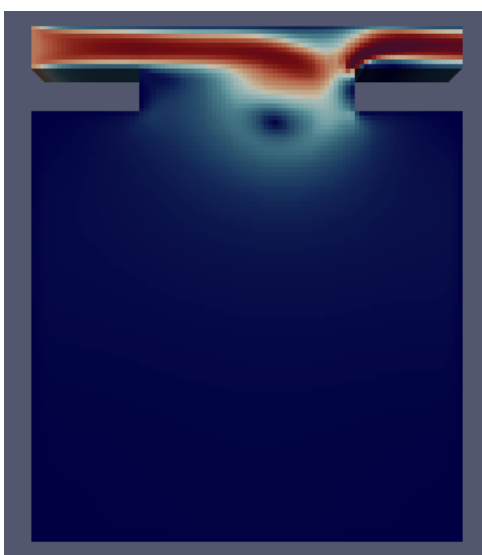
Plots will be shown in the following order: P, U, UX, UY, P-contour, U-contour, UX-contour, UY-contour, Streamlines for T=60.

Re=1000

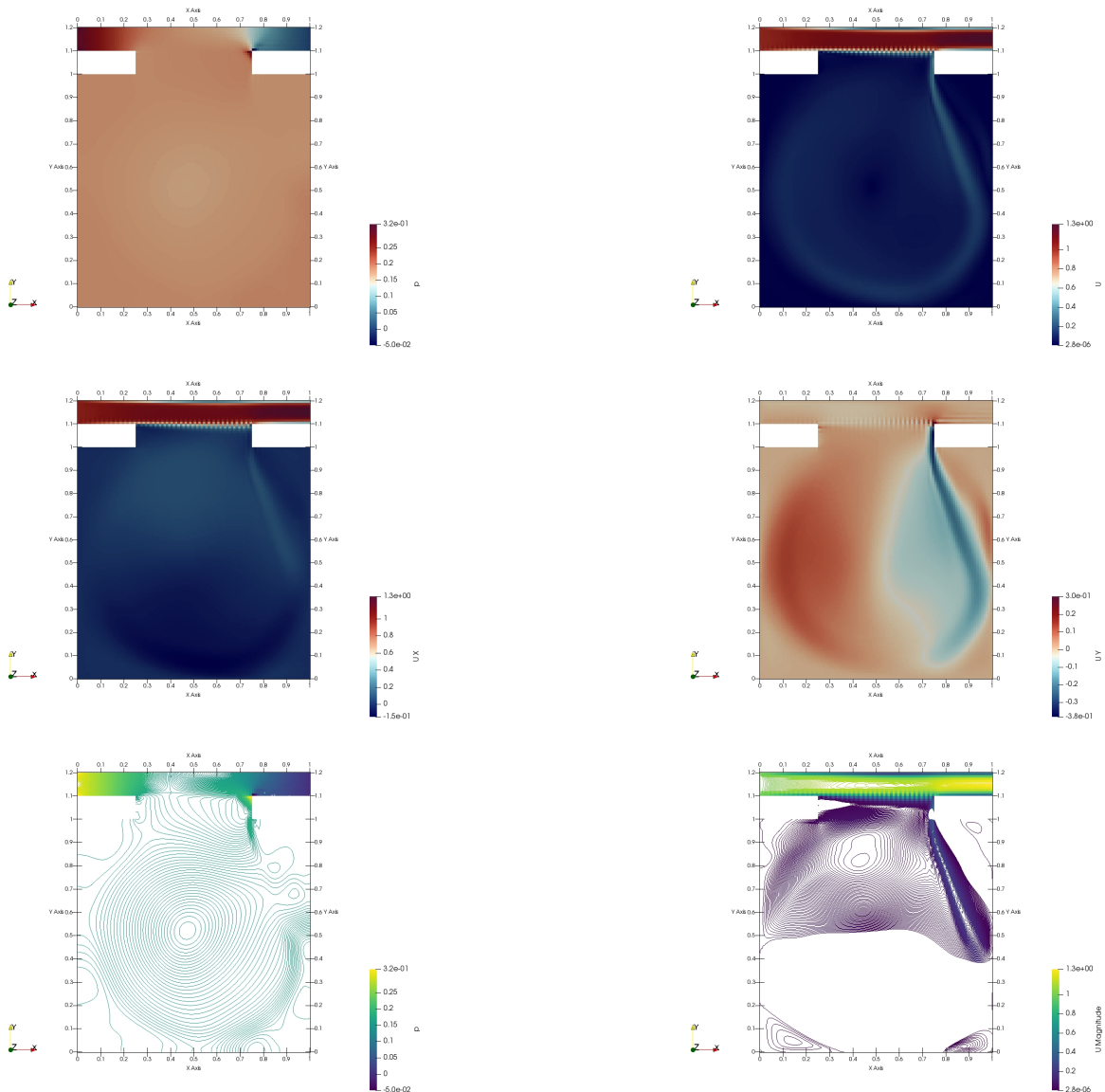


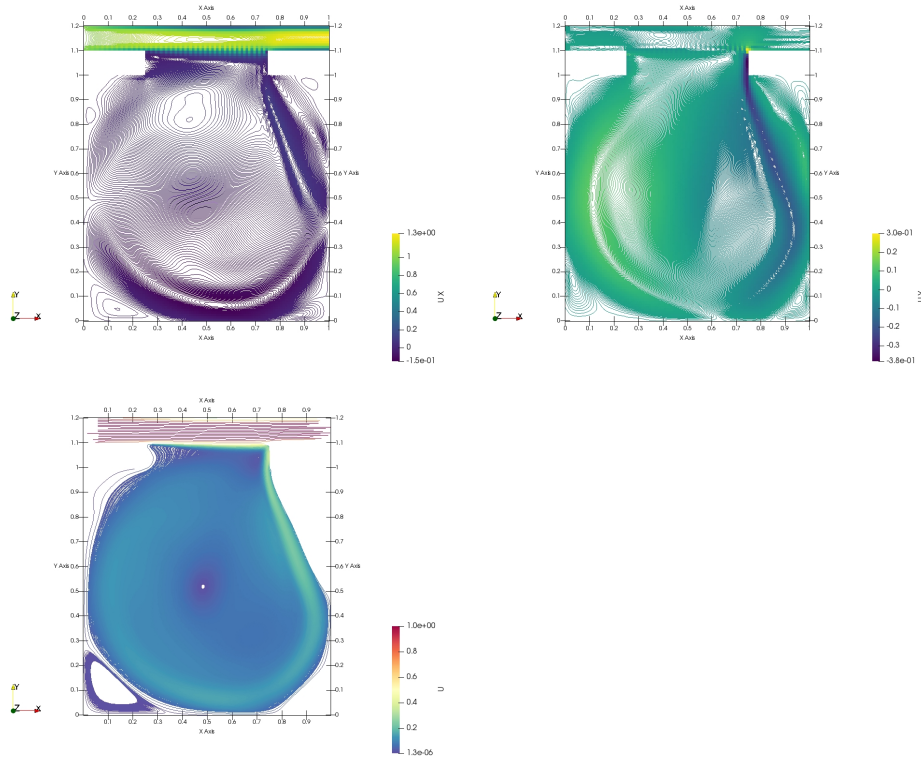


Re=1000, U at T=1,2,6

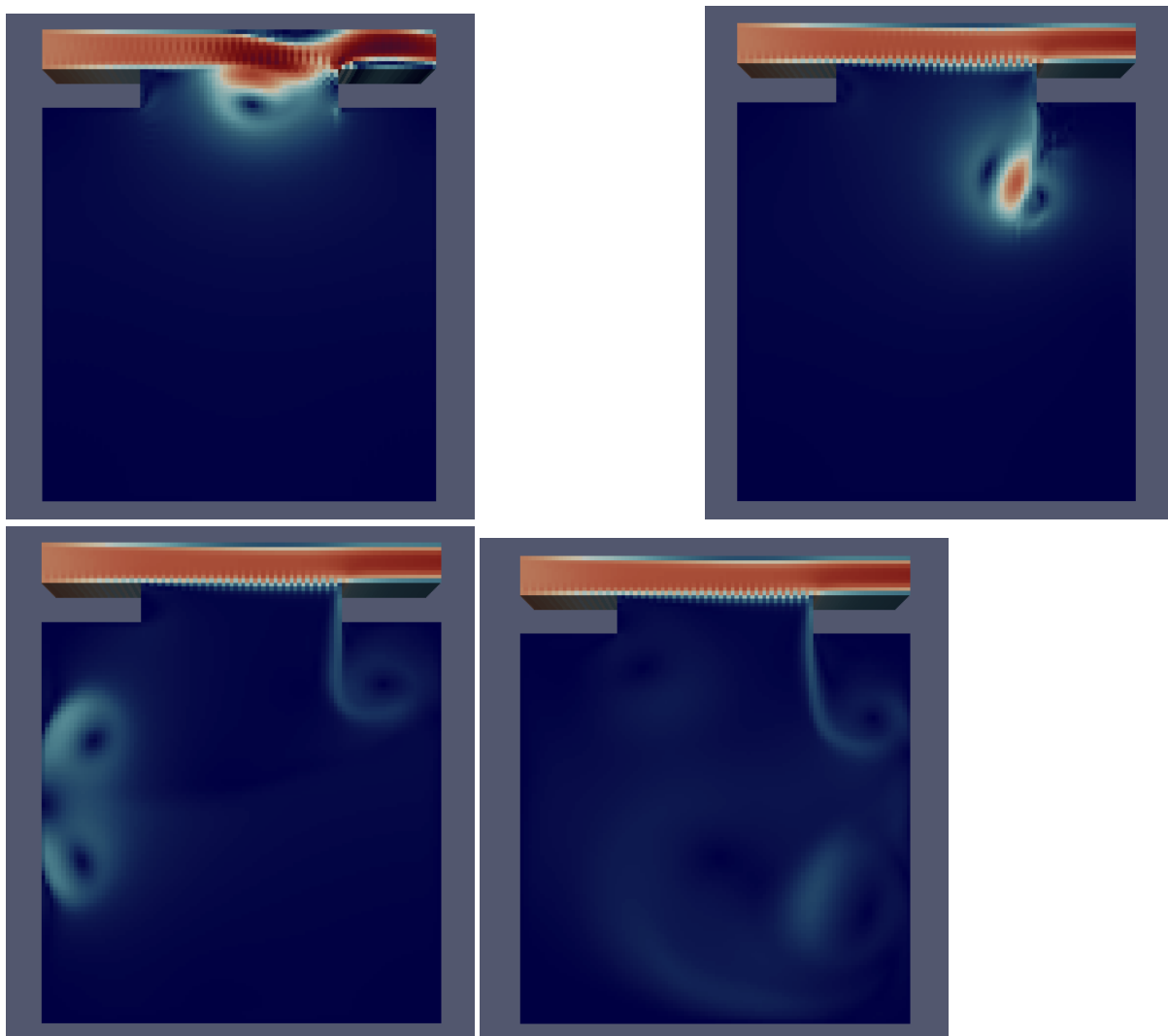


Re=10000





Re=10000, U at T=1,2,6,30



6.9. Vortice Positions

Convergence can again easily be seen by looking at the centralized vortex position for both meshes, by differing geometry.

meshfactor	Reynolds	window.a.	wall.w.	Vortex.Center.Location.along.Y
3	1000	0.5	1	0.691667
5	1000	50.0	1	0.705000
3	10000	0.5	1	0.641667
5	10000	50.0	1	0.595000

Table 5:

6.10. Strouhal Number and Vortex Shedding

We will now look at the frequency of the vortex shedding that occurs at the right window wall. In non-dimensional form (in terms of L/U), this is the Strouhal number.

Two probes are placed 0.025 to the left and right of the right vertical wall, 0.05 below the lower edge. We will denote the left probe as probe 0, and the right probe as probe 1.

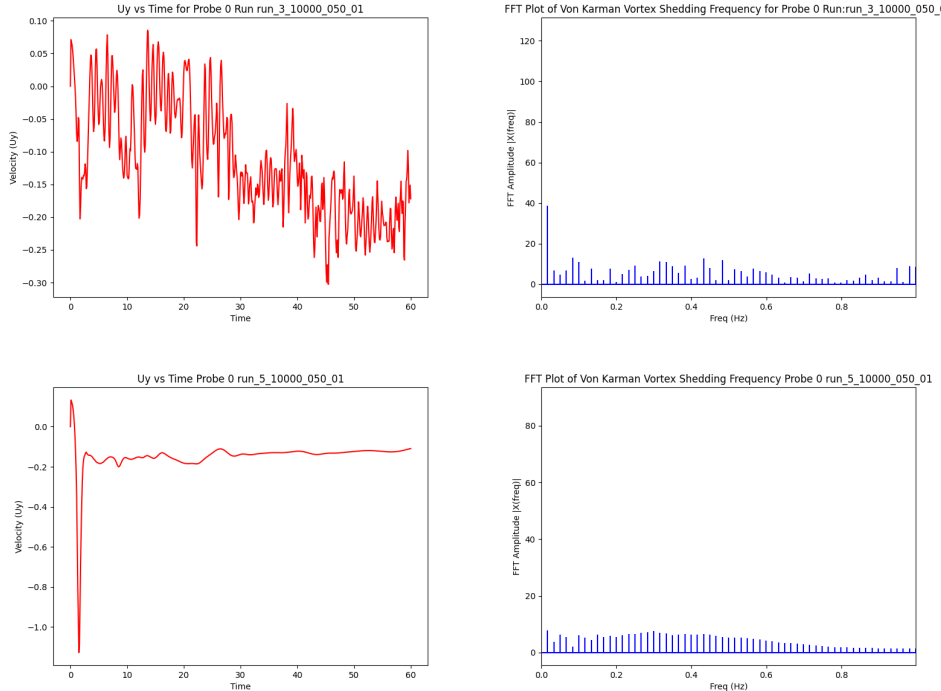
Coarse meshes will be shown along with their refinements.

Fast Fourier Transform (over all time)

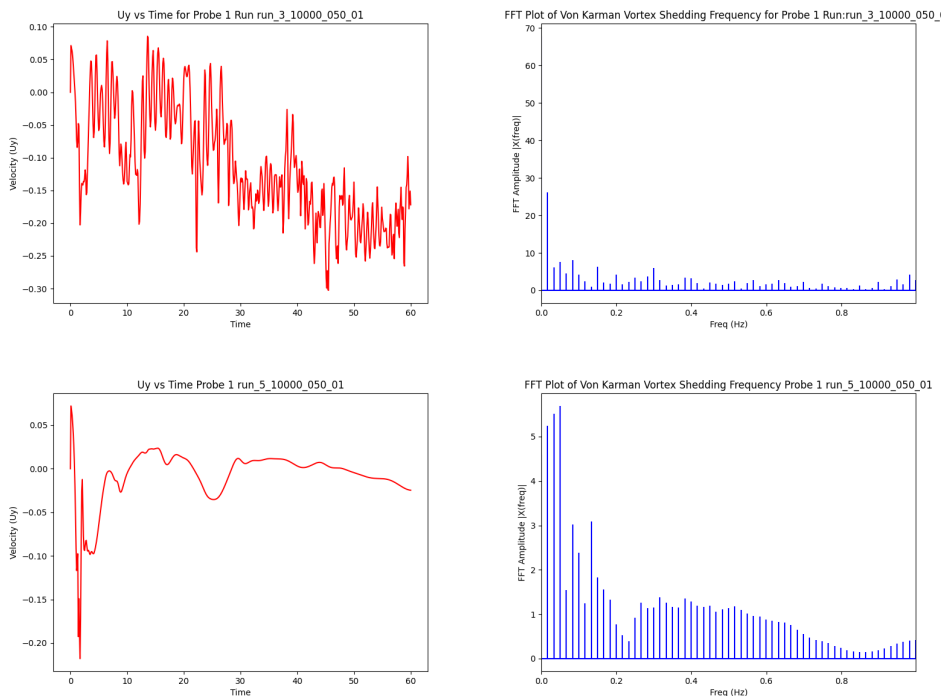
From the images shown earlier, clearly there is no vortex shedding for the $Re=1000$ case, and it seems to stabilize quickly, so one might assume that the flow is steady.

Below we have only treated the $Re=10000$ case, since the $Re=1000$ case does not produce useful filtered output (which might seem to corroborate the above).

Re=10000, Probe 0



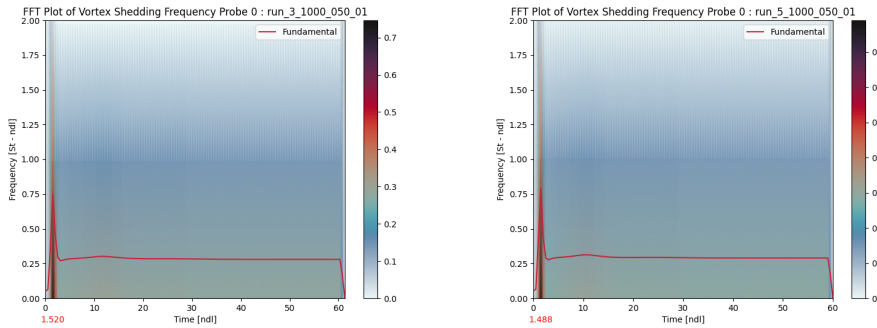
Re=10000, Probe 1



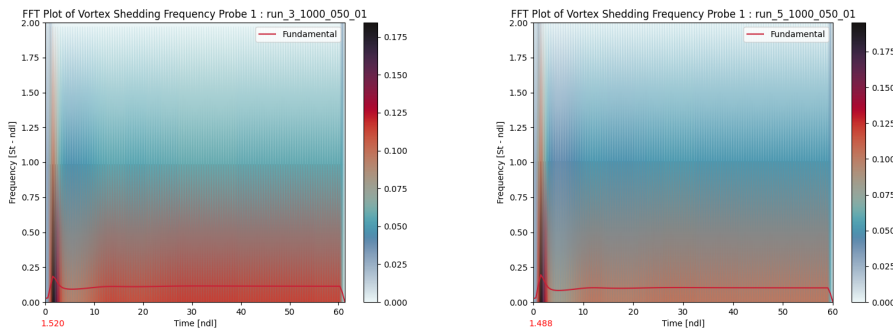
Note that the meshFactor of 3 fails to capture solution behavior (see the added oscillation).

Short Time Fourier Transform (spectrogram to see time evolution)

Re=1000, Probe 0



Re=1000, Probe 1

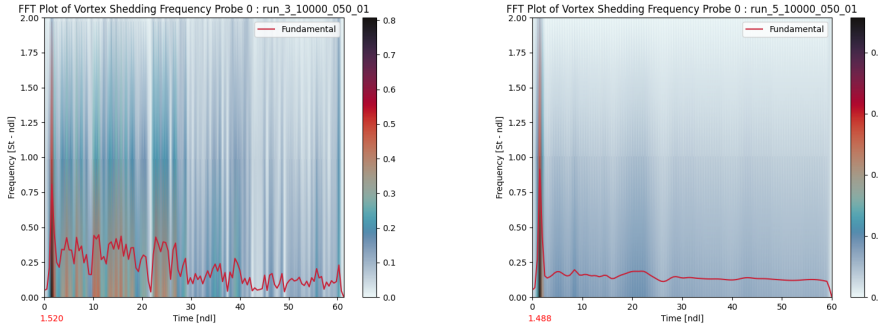


Interestingly, the Re=1000 plot is not at 0 Strouhal number! So we can clearly see that the large-scale flow does not have any steady-state oscillation (which is what the previous FFT plots show), but the small-scales are unsteady, with a typical Strouhal number near 0.2, as seen in the later table.

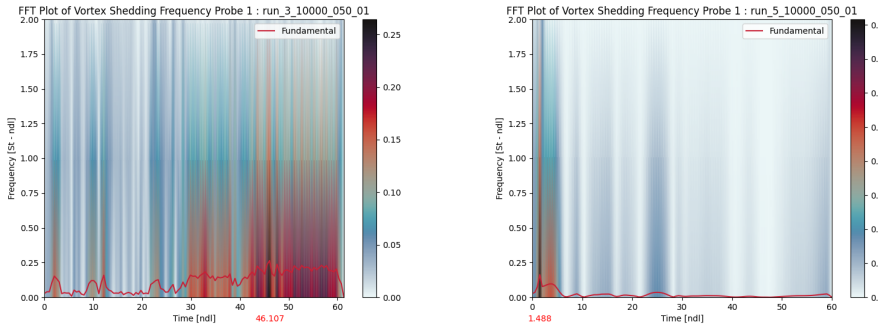
This is confirmed by the following:

For spheres in uniform flow in the Reynolds number range of $8 \times 10^2 < \text{Re} < 2 \times 10^5$ there co-exist two values of the Strouhal number. The lower frequency is attributed to the large-scale instability of the wake, is independent of the Reynolds number Re and is approximately equal to 0.2. The higher-frequency Strouhal number is caused by small-scale instabilities from the separation of the shear layer. ([Kim and Durbin 1988](#); [Sakamoto and Haniu 1990](#))

Re=10000, Probe 0



Re=10000, Probe 1



Continuing the former analysis, we see that the large scale instabilities are independent (since we get another Strouhal number for $Re=10000$ near 0.2 later in the flow). On the other hand, the small-scale instabilities are more prominent here, in the form of disturbances to the transform. We do not capture the other Strouhal number due to placement of the probes; we are interested in the large scale flow, so the other Strouhal number is not relevant for this paper.

Note again that the meshFactor of 3 is insufficient to capture the solution.

Equilibrium Large-Scale Strouhal Values

Note that transient Strouhal numbers exist for $Re=1000$, and there are also small-scale Strouhal numbers for $Re=1000$, but those are neither relevant nor easily retrievable for this study.

meshfactor	Reynolds	ProbeNumber	Strouhal
3	10000	0	0.116472
3	10000	1	0.166389
5	10000	0	0.316139
5	10000	1	0.149750

Table 6:

Note the stark difference between left and right frequencies - the higher one may be the second Strouhal number mentioned in the previously cited articles.

7. High Reynolds Number - Part 2

7.11. Window Wall Solution Profiles

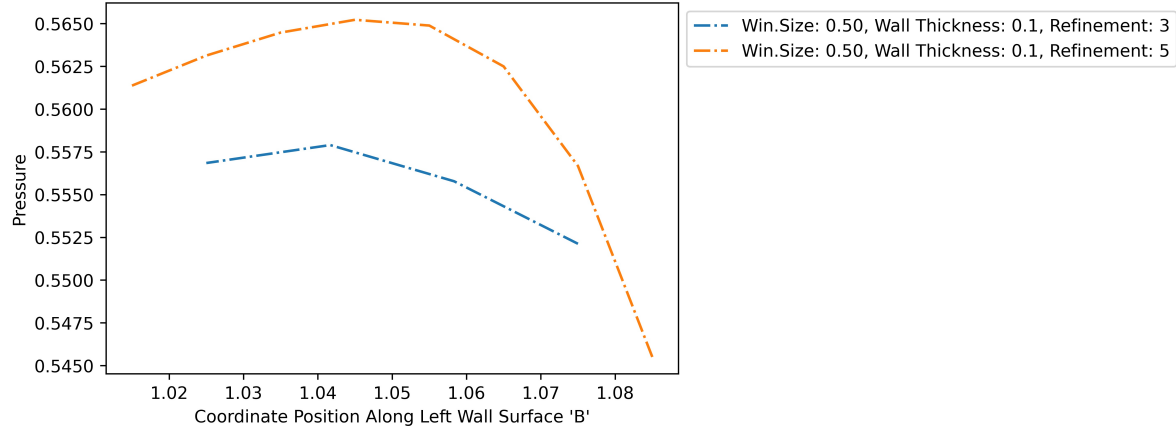
Now consider again the profiles along the left and right window walls; the vertical segments along the inside of the window.

This time we will consider the starting behavior of these profiles at high Re, in particular between T=1 and 2.

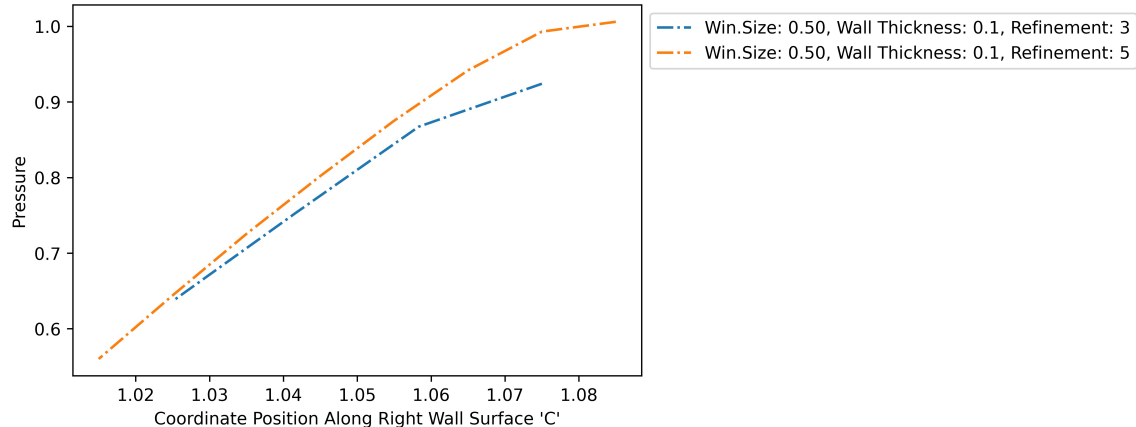
T = 1.3 (unsteady startup)

Re=1000

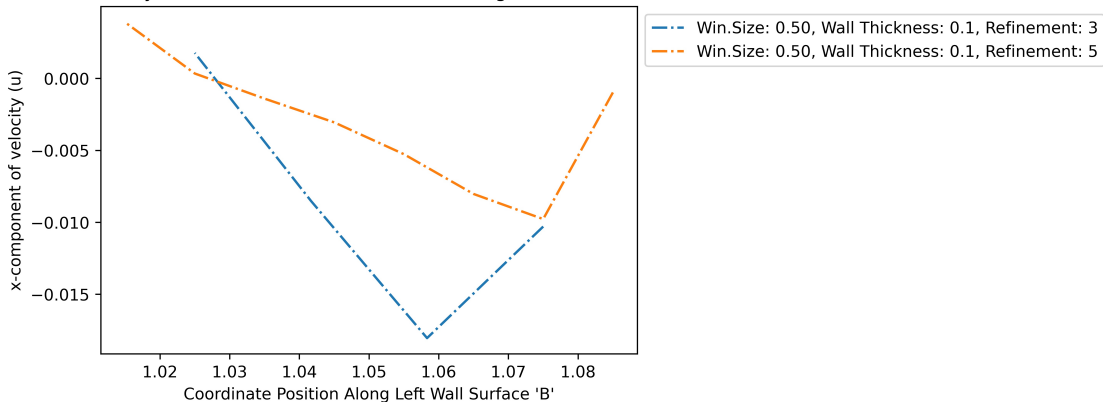
Pressure vs Position at t = 1.3 seconds Along Left Wall Surface for Re = 1000

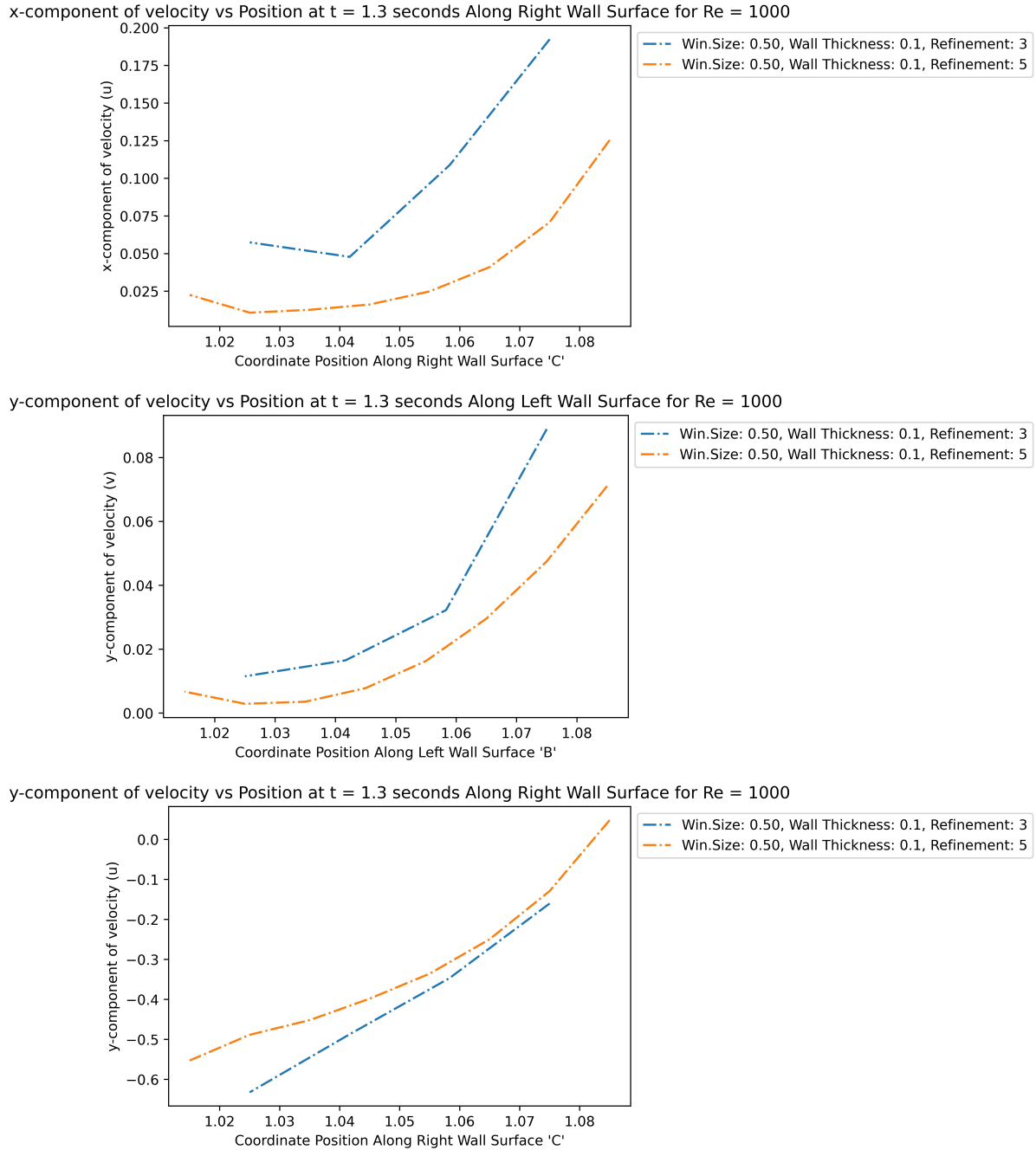


Pressure vs Position at t = 1.3 seconds Along Right Wall Surface for Re = 1000

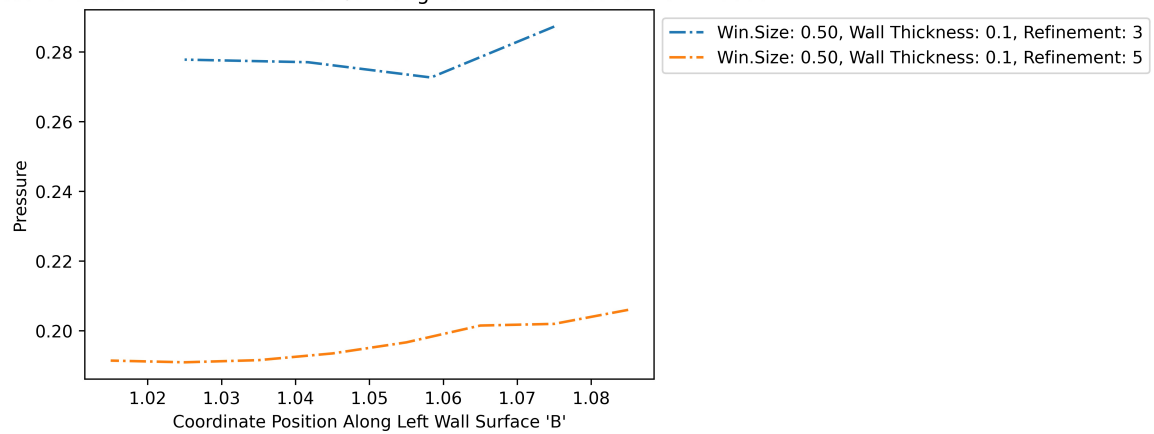
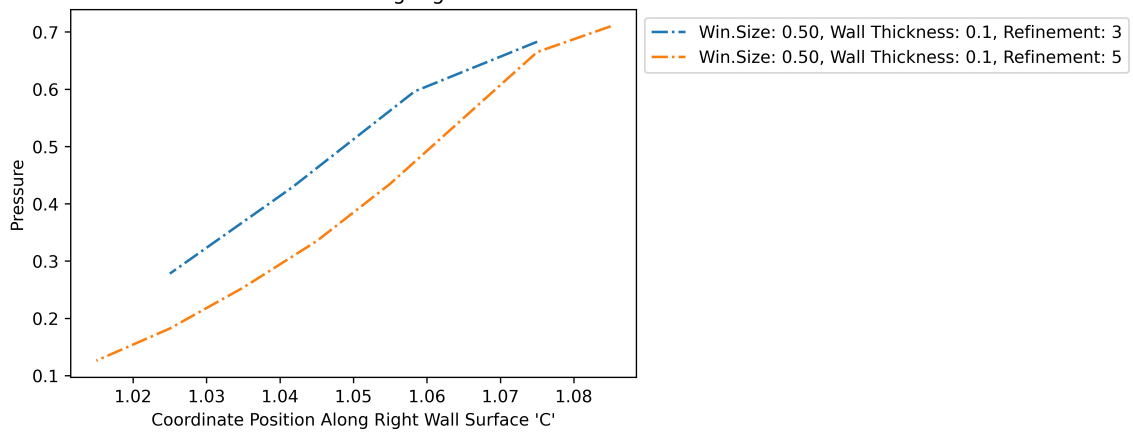
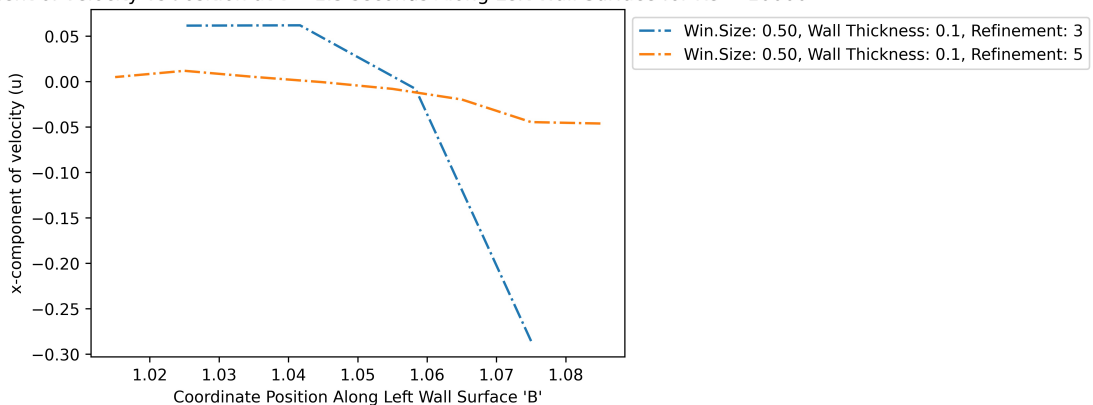


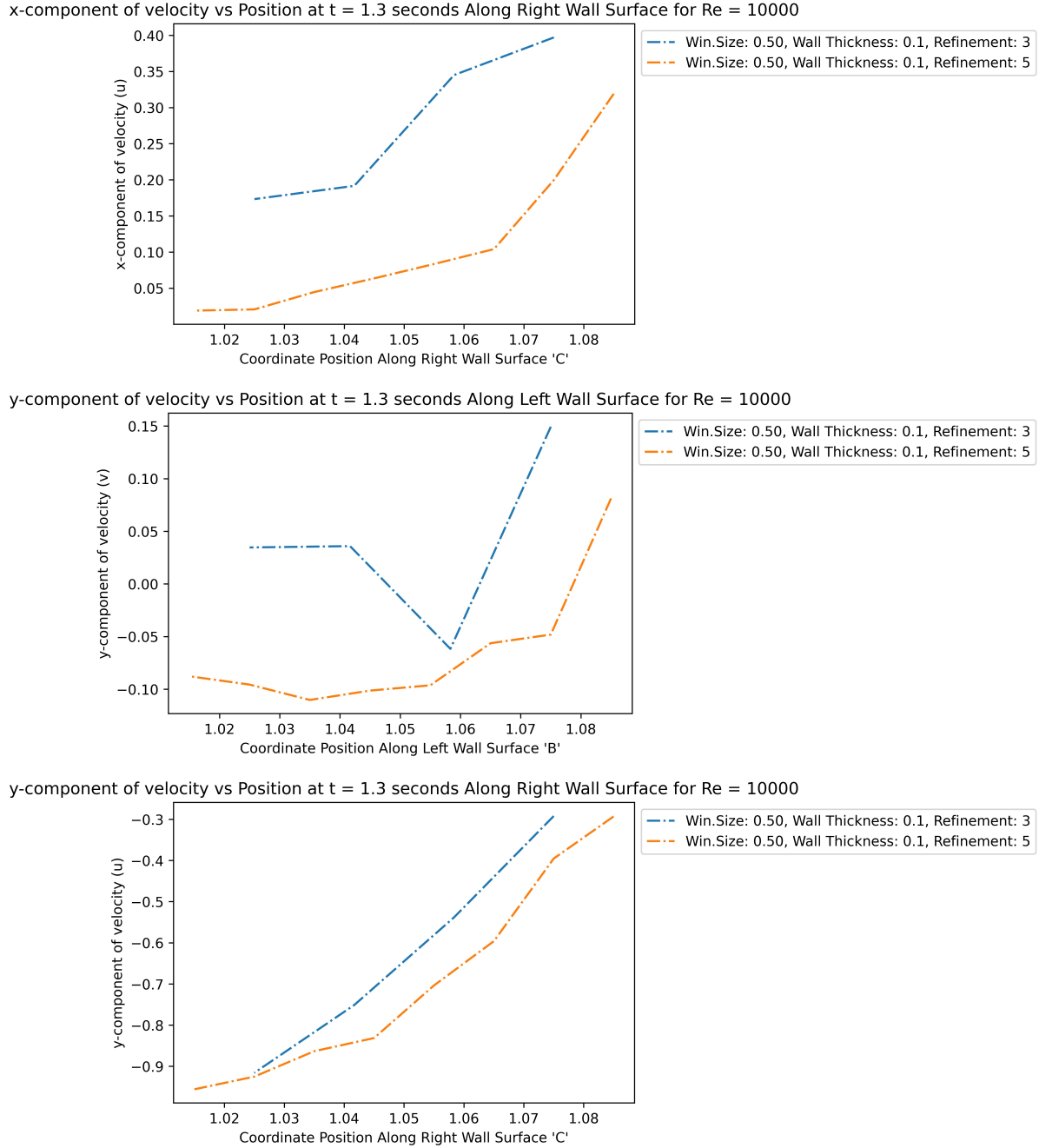
x-component of velocity vs Position at t = 1.3 seconds Along Left Wall Surface for Re = 1000





Re=10000

Pressure vs Position at $t = 1.3$ seconds Along Left Wall Surface for $Re = 10000$ Pressure vs Position at $t = 1.3$ seconds Along Right Wall Surface for $Re = 10000$ x-component of velocity vs Position at $t = 1.3$ seconds Along Left Wall Surface for $Re = 10000$ 



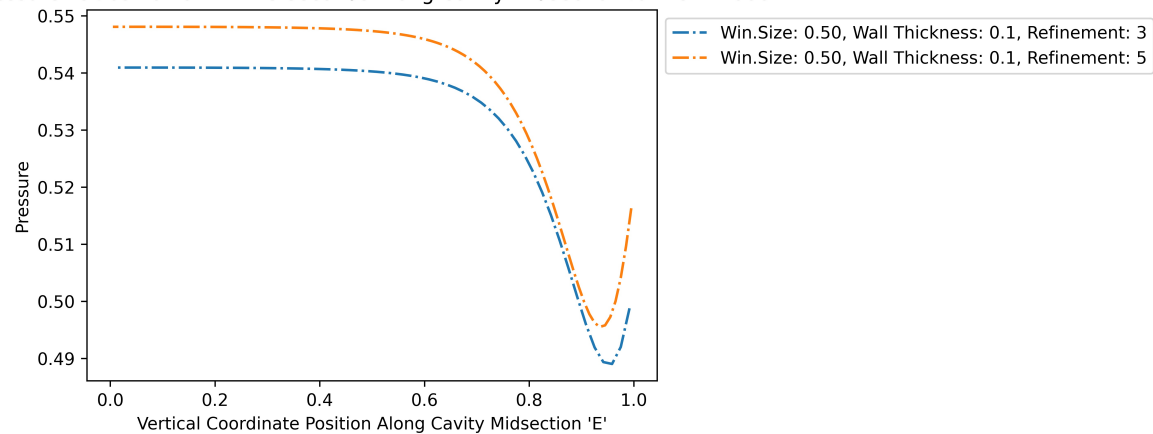
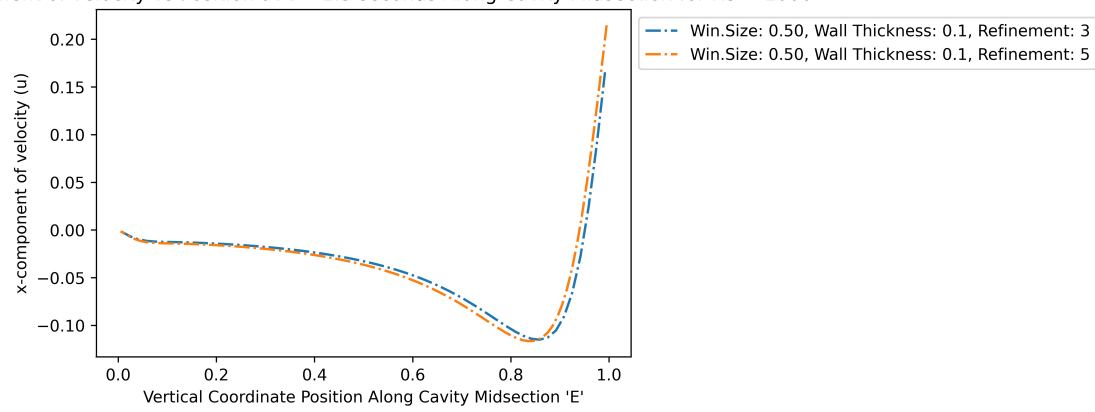
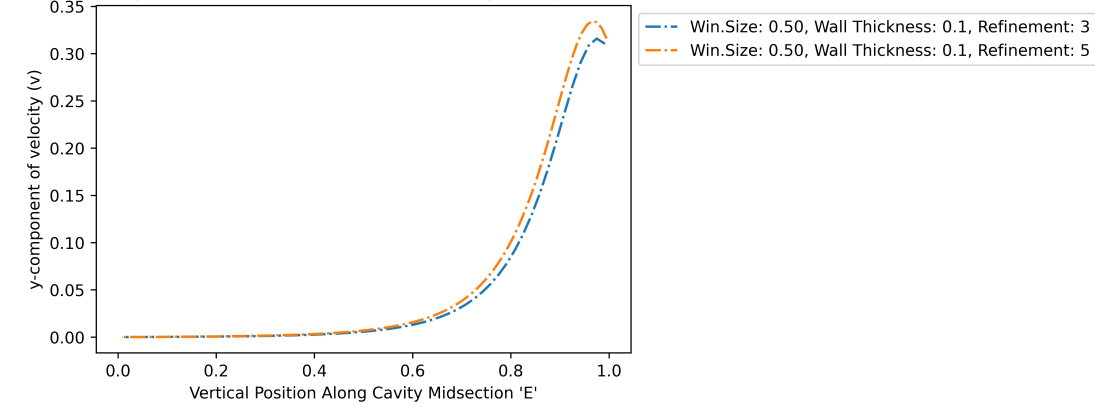
Maximum Strain Rate over Time

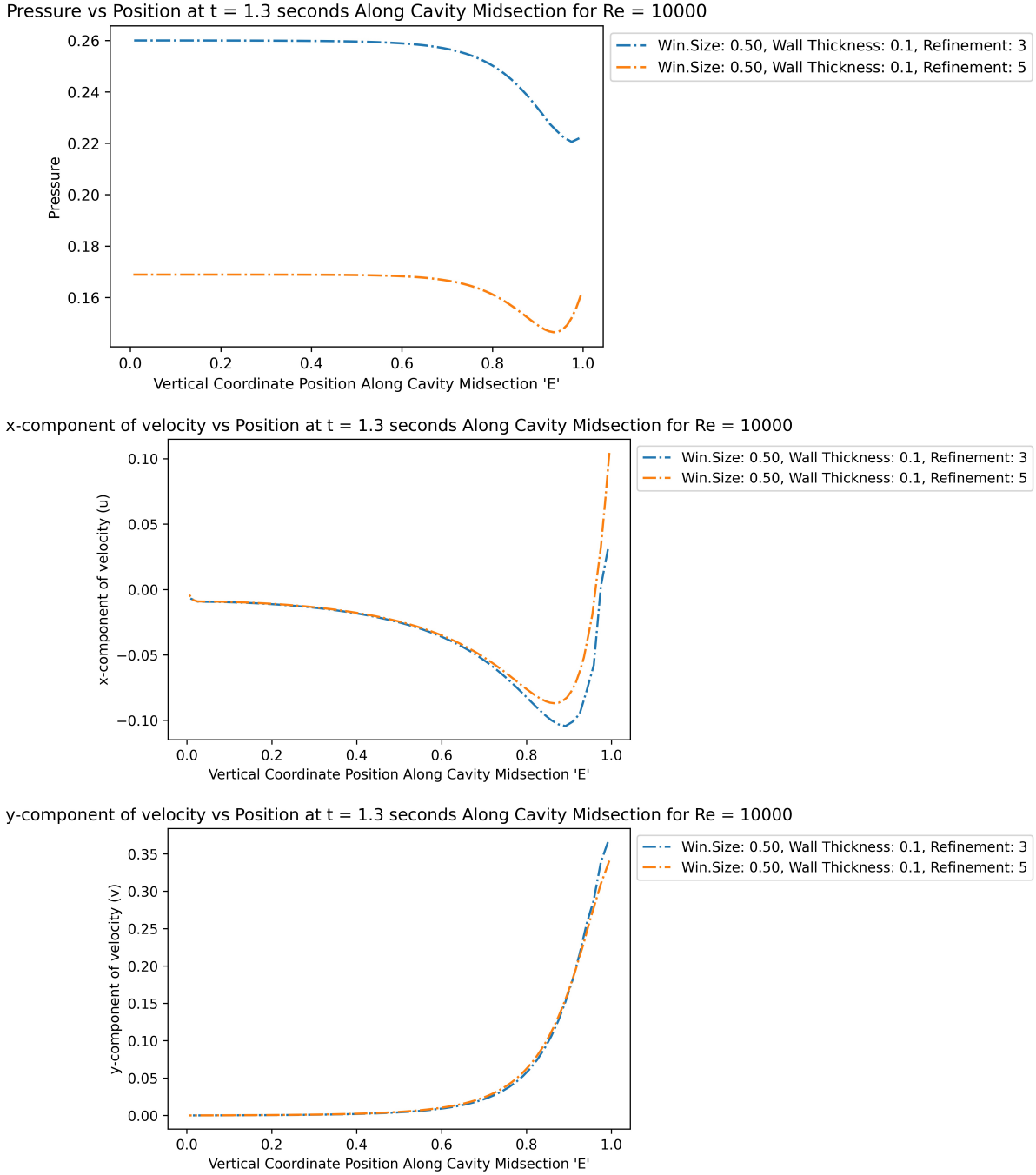
TBD

7.12. Cavity Midline Solution Profile

Now again consider the profiles along the vertical midline down the cavity; from the middle of the window down to the back of the cavity.
Similarly, we will only consider T=1.3.

Re=1000

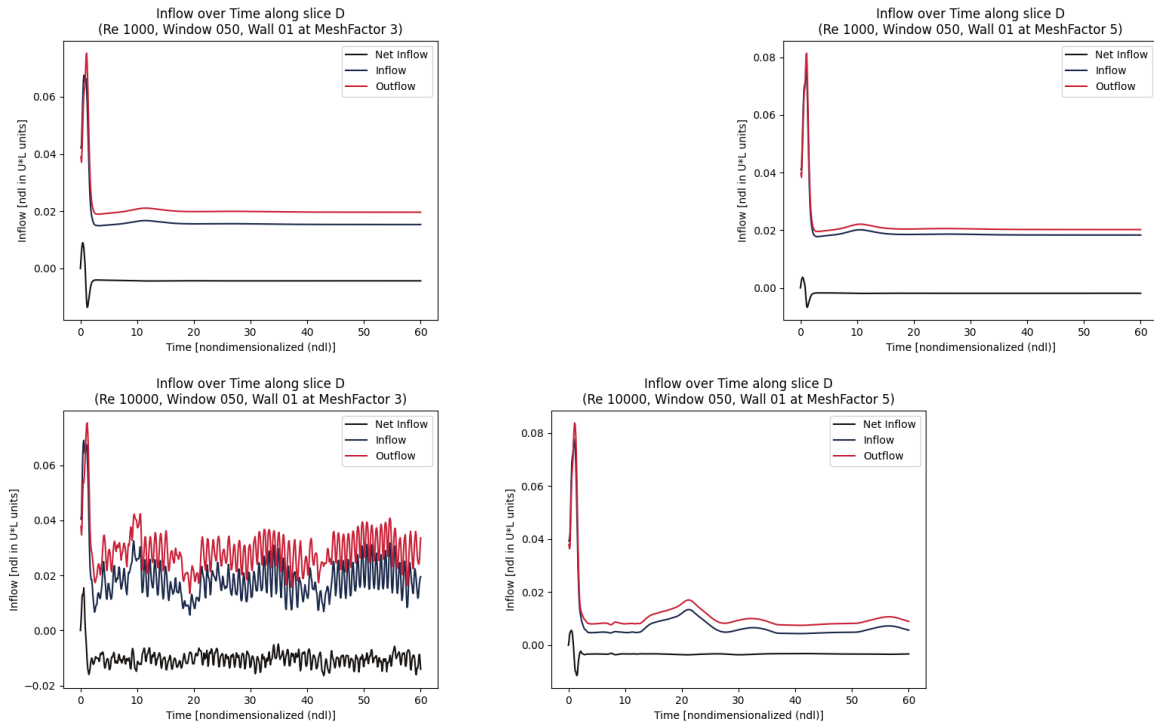
Pressure vs Position at $t = 1.3$ seconds Along Cavity Midsection for $Re = 1000$ x-component of velocity vs Position at $t = 1.3$ seconds Along Cavity Midsection for $Re = 1000$ y-component of velocity vs Position at $t = 1.3$ seconds Along Cavity Midsection for $Re = 1000$ **Re=10000**



7.13. Volumetric Flow Rate and Mixing

To investigate inflow/outflow rates, we will consider integration of a profile across the internal window opening (profile D on the mesh diagram).

Note that the meshFactor of 3 fails for $Re=10000$ again.



Looking at the net flow rate, clearly the cavity first pressurizes and then slowly depressurizes over time.

While this is happening, large amounts of fluid are still being cycled through the window - a huge amount in the first few timesteps (up to $\sim T=2$), and then a somewhat large amount afterwards.

To visualize the scale, an example will be shown.

For a $1m^2$ window and $90km/hr(56mph)$ wind, approximately $(25m/s)(1)(1)(0.08) = 2m^3/second$ is cycled through in the first ~ 2 seconds!

Afterward, $0.25m^3/s$ is cycled in and out on average.

After the initial spike, there is a net decreasing outflow starting at $0.05m^3/s$ (using the Re=10000 plot).

Note this example is fairly realistic, since an EF0 tornado has slightly higher windspeed, and can be approximated as parallel streamline flow due to the large tornado radius.

While this example is not entirely accurate since the windspeed used can produce much higher Reynolds numbers in flow, the large-scale behavior is identical, as shown below.

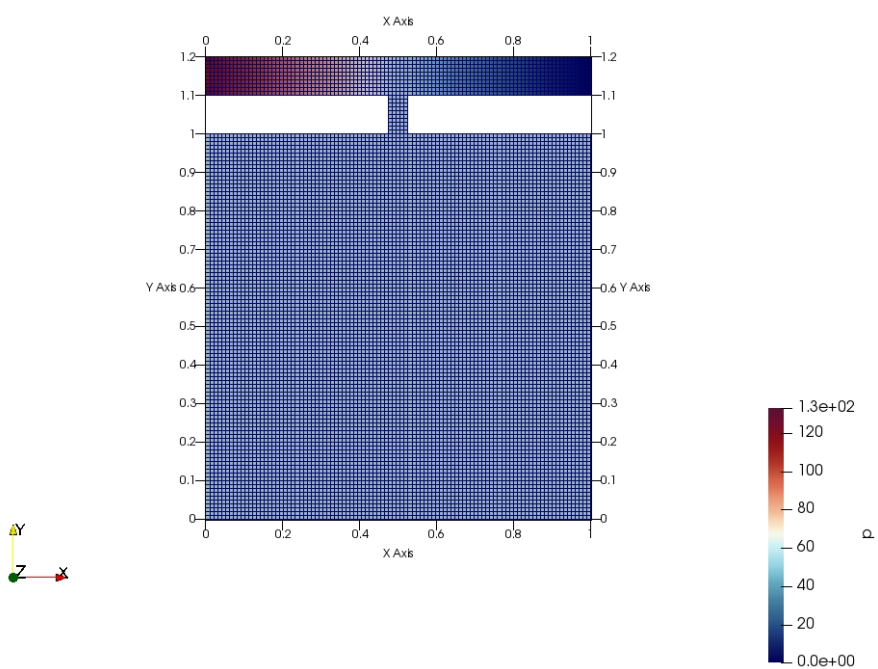
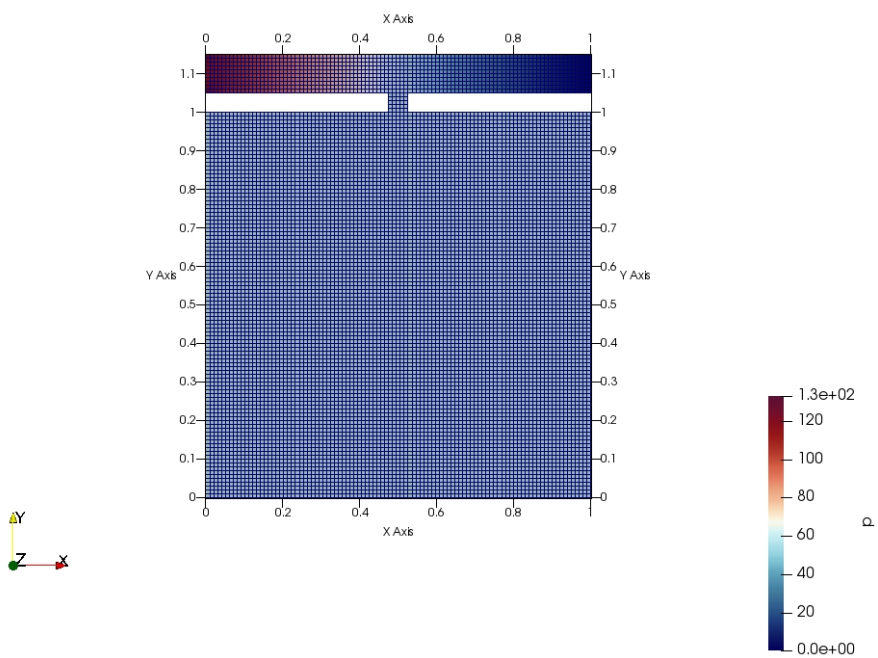
Note that the maximum cycle flow rate of 8% freestream is consistent between both Reynolds numbers. From the previous analysis on Strouhal numbers, we see that since the large-scale flows are fairly Reynolds-number-independent, it is possible that the volumetric flowrate has converged, and will remain the same for higher Reynolds numbers.

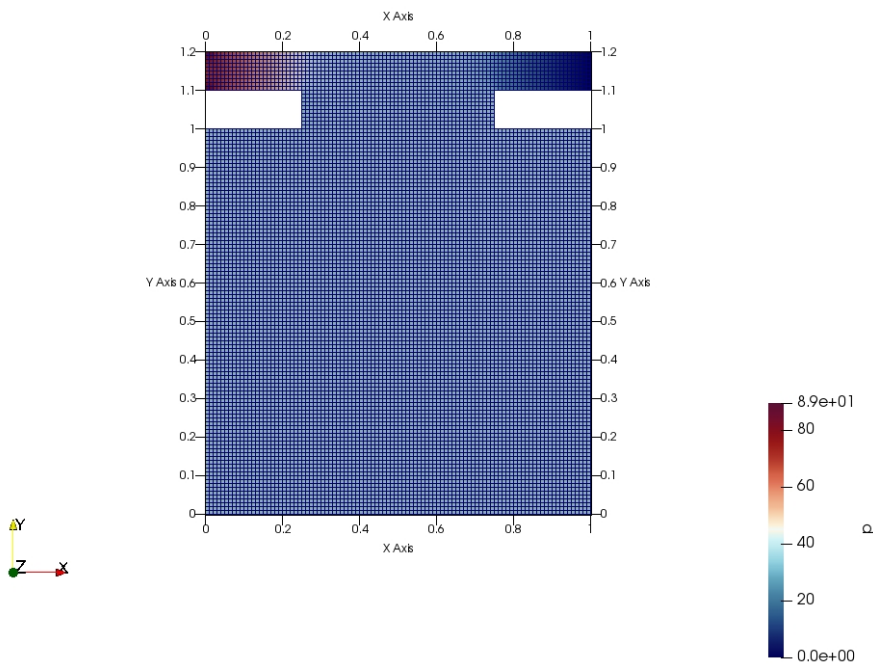
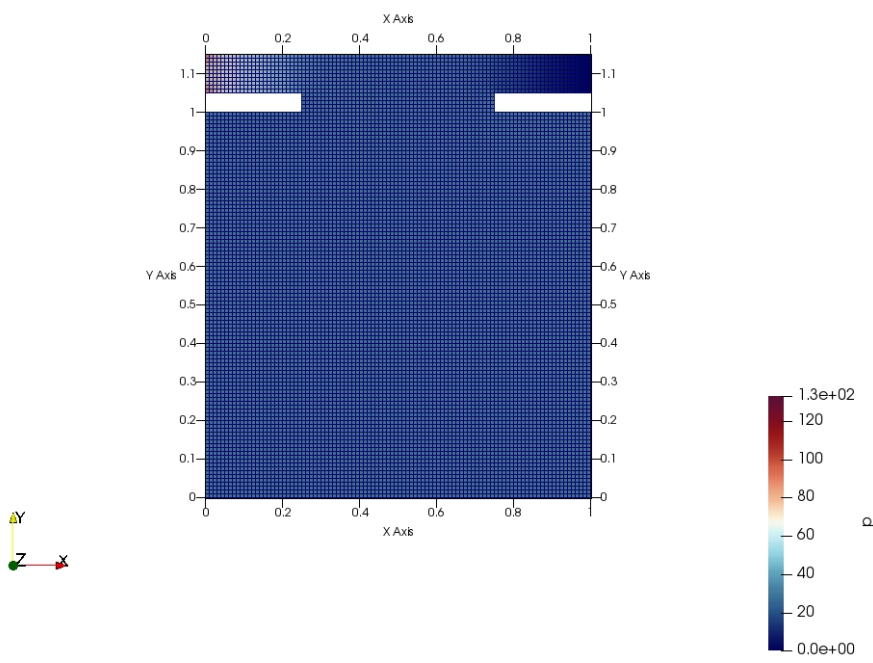
If that is the case, then the low-Reynolds analysis can be combined with a couple of measurements of high-Reynolds flow, and extrapolated out to actual cases, providing an extremely useful tool for flow estimation.

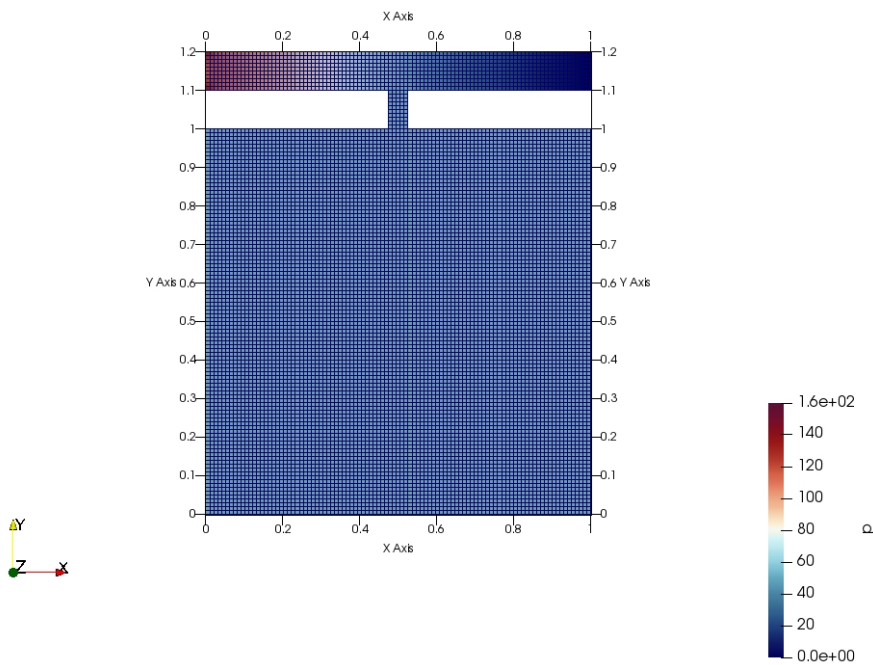
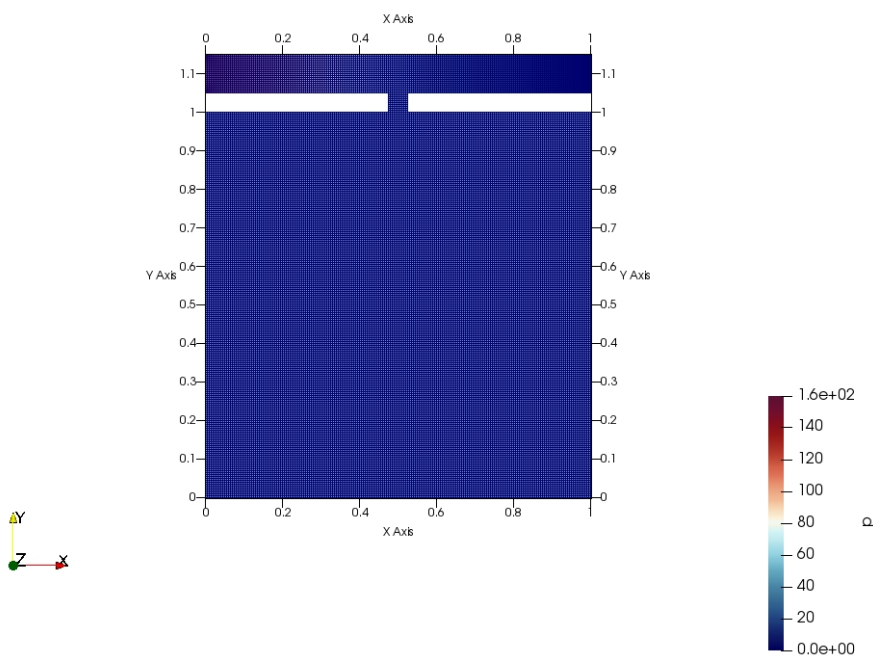
8. Appendix

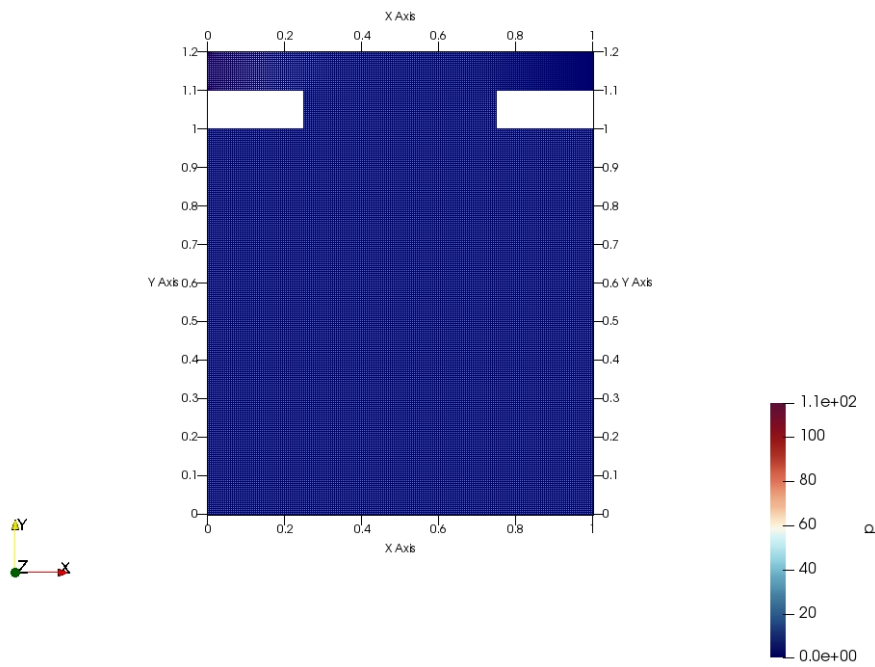
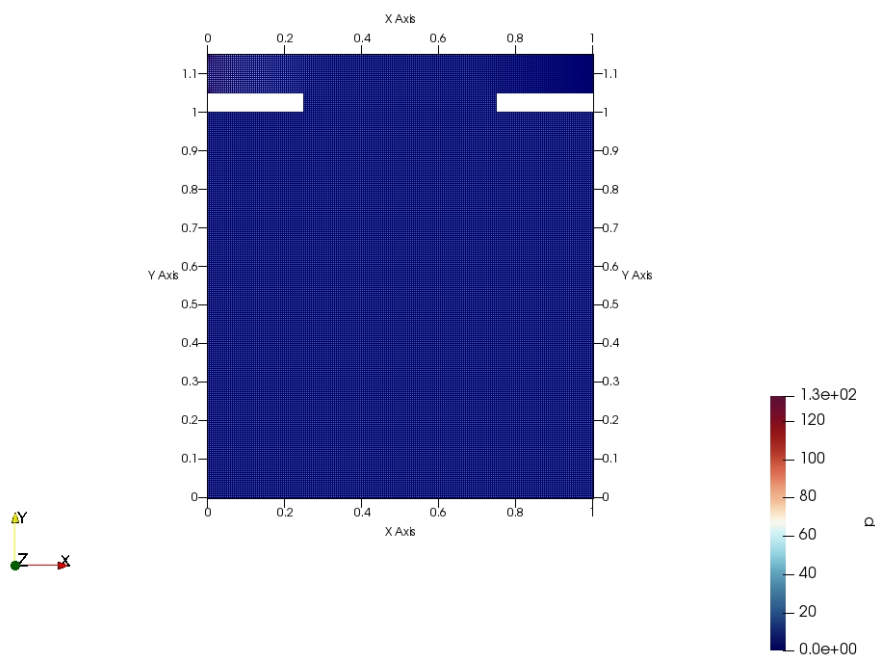
8.14. Mesh Images

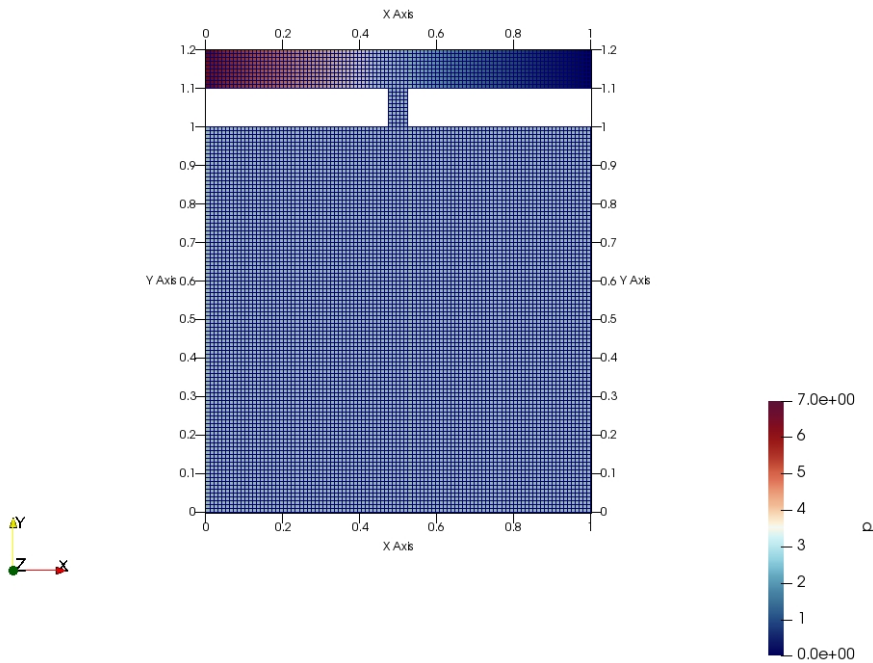
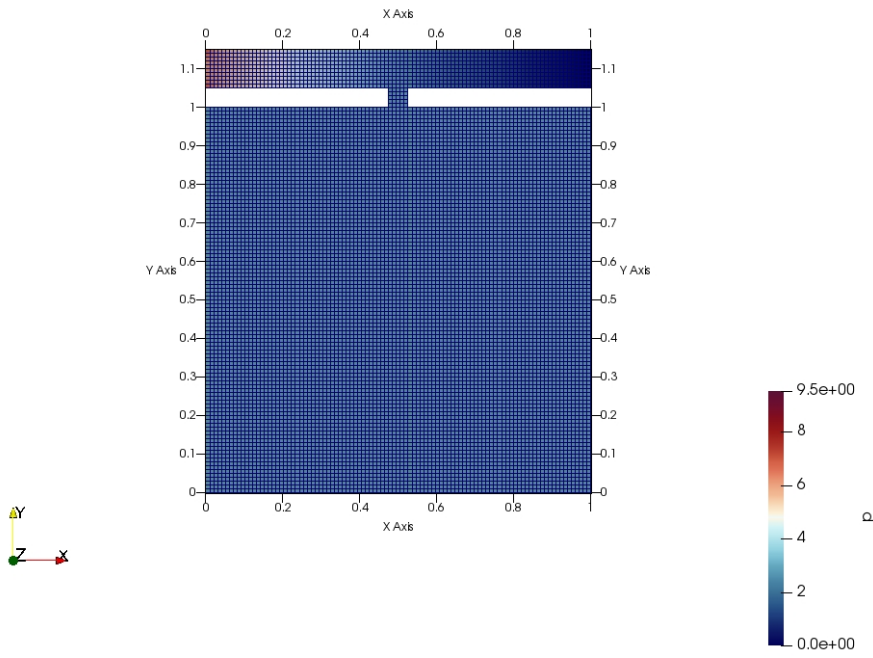
Mesh Images for the Low Reynolds simulations (same order)

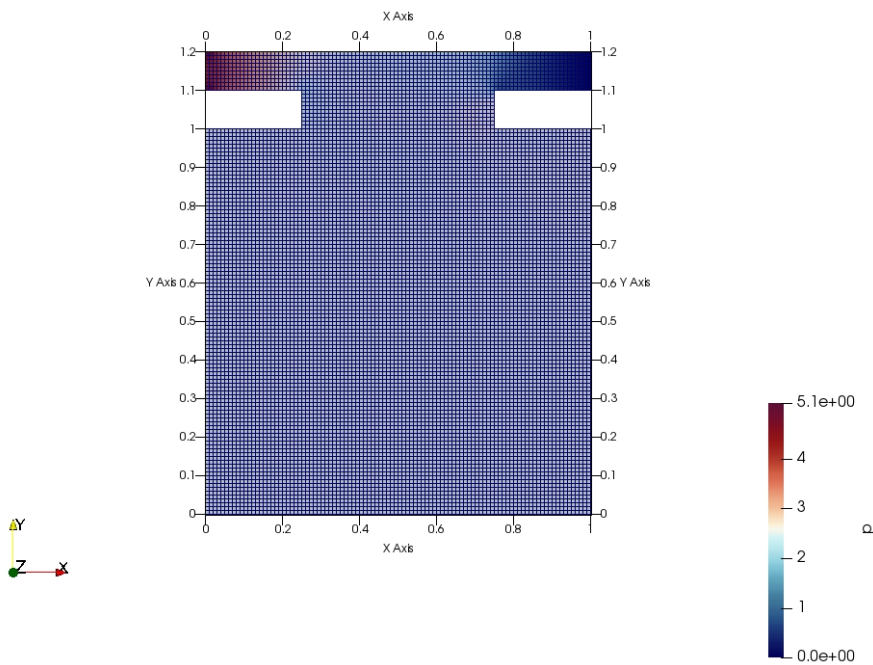
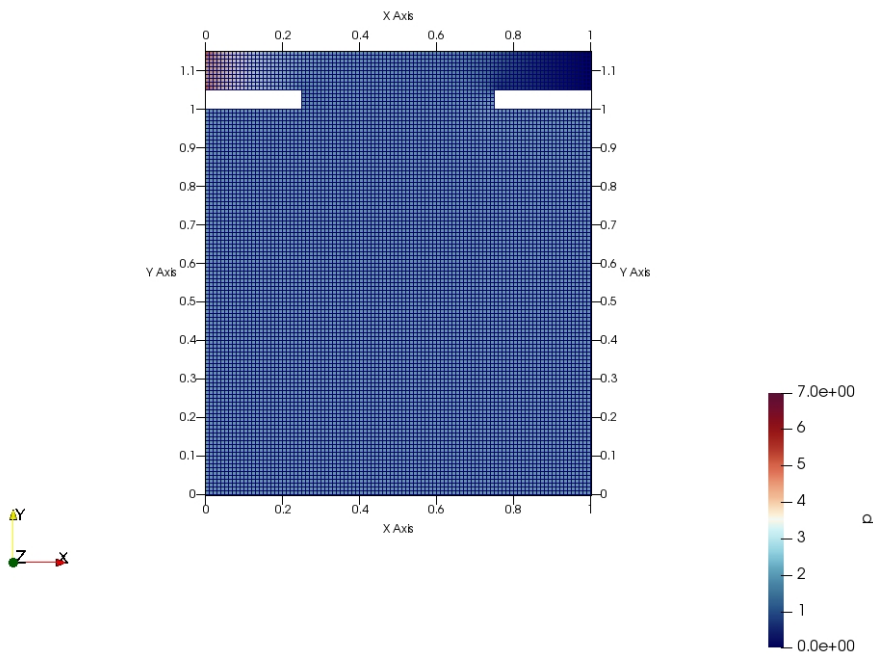


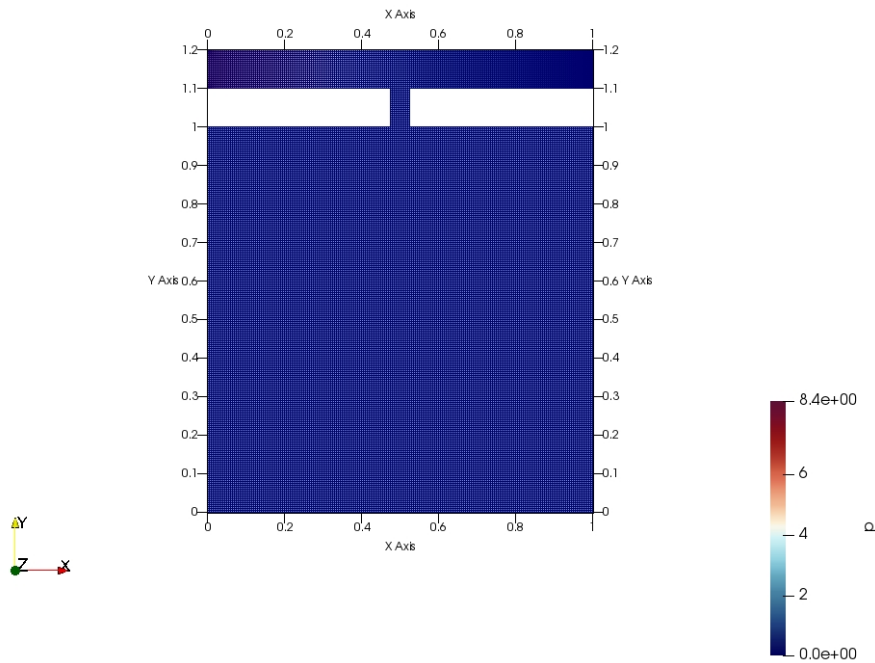
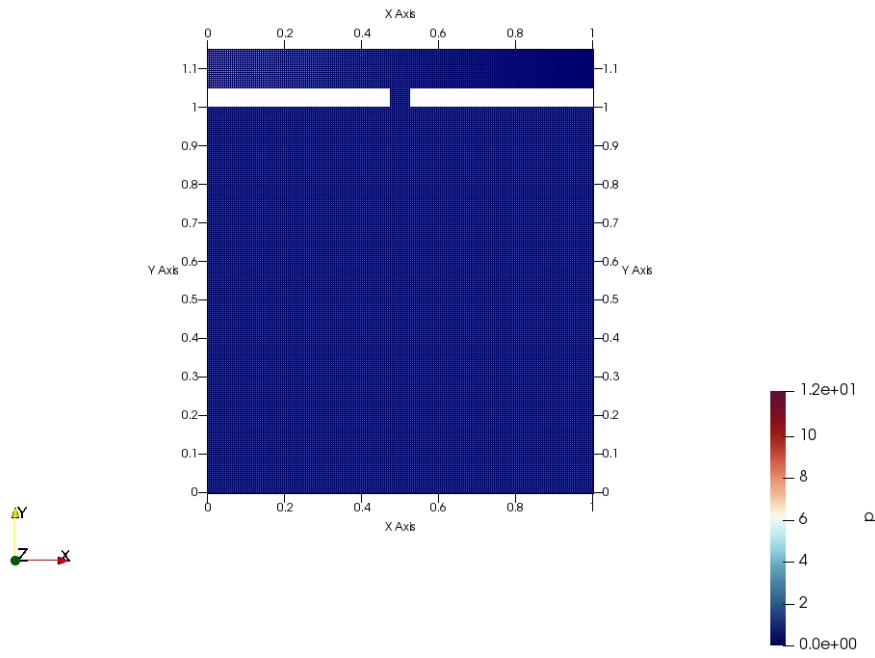


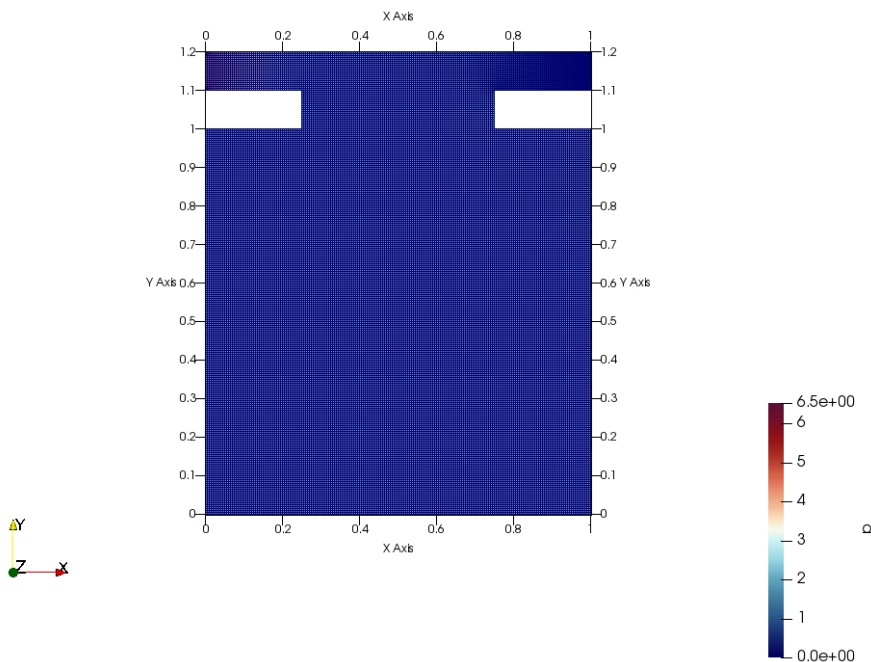
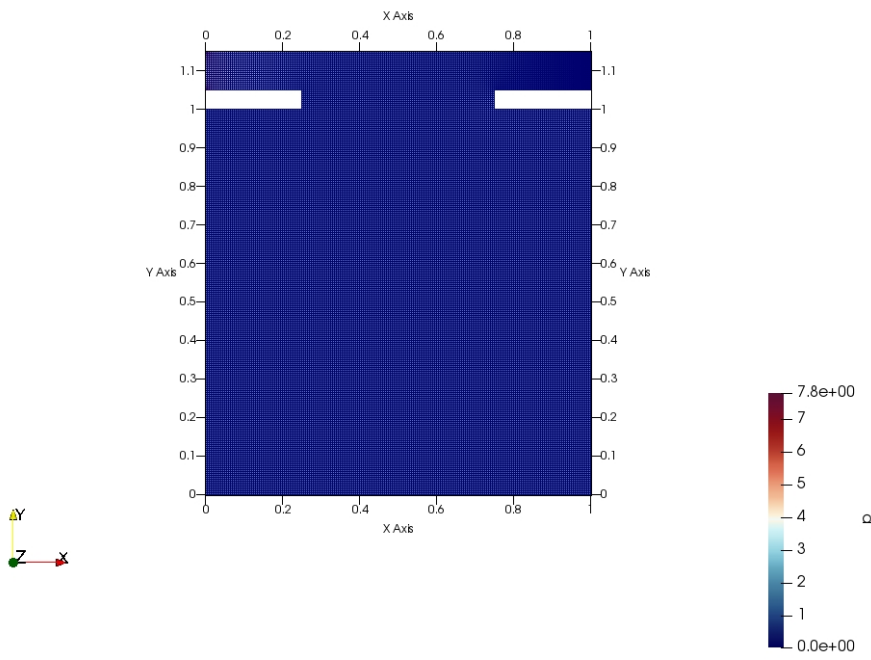




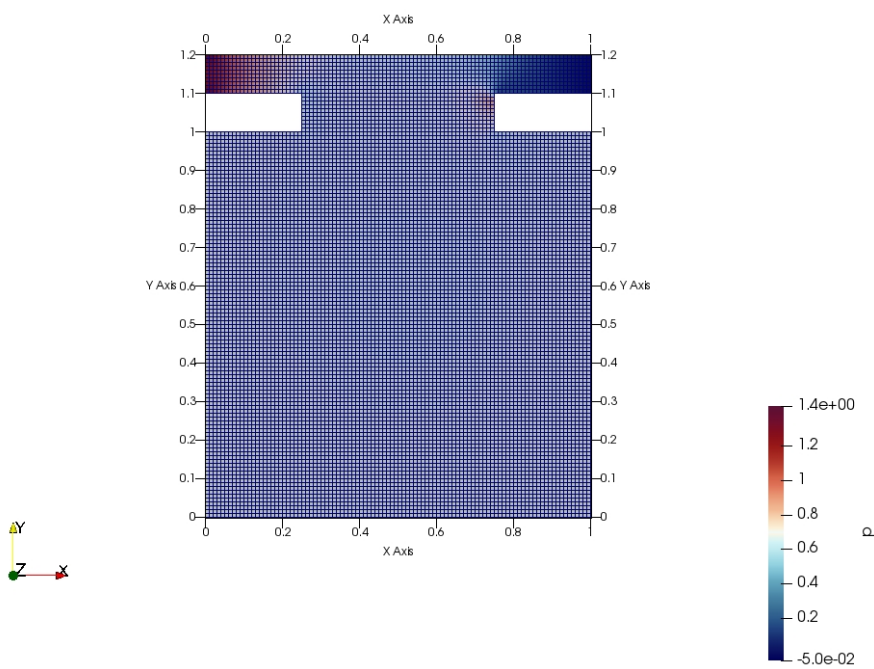
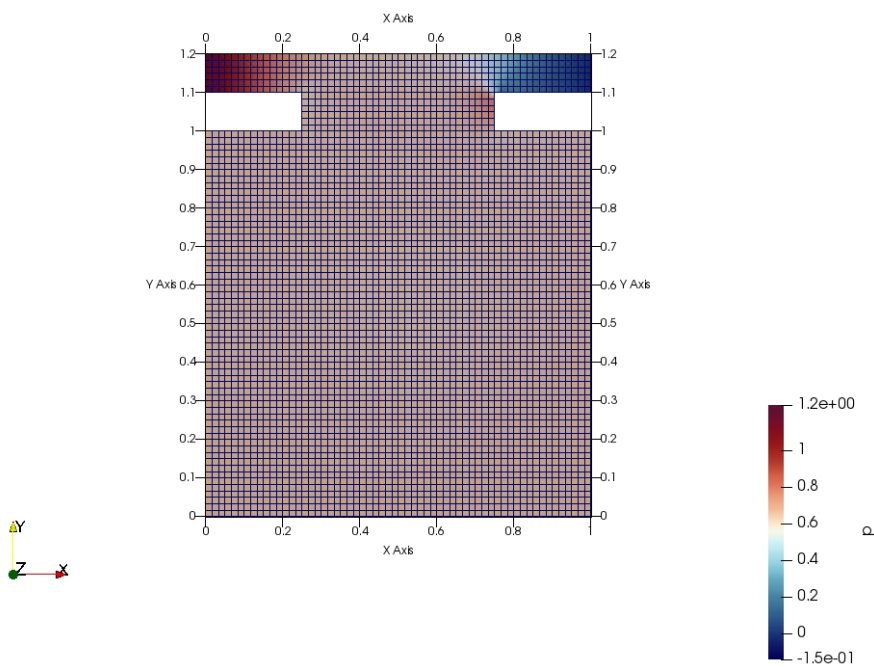


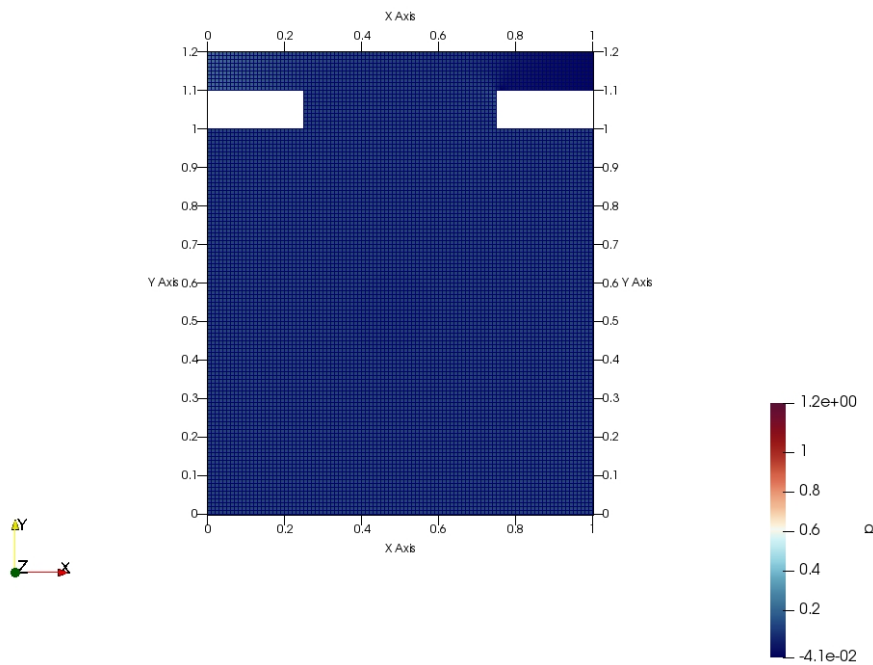
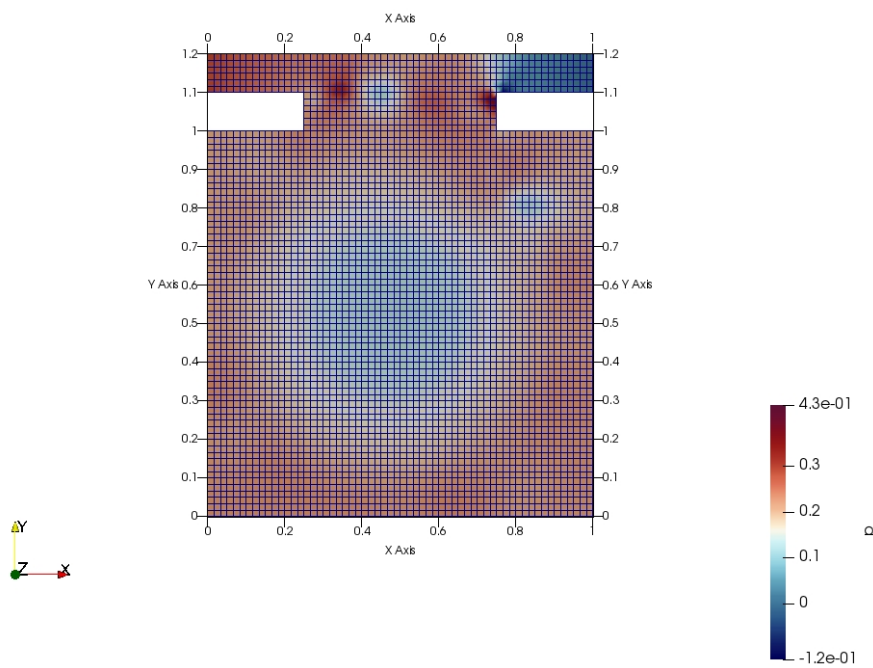






Mesh Images for the High Reynolds simulations (same order)





9. References

(2019, May). *Super Inspection Pros*. Retrieved from <https://superinspectionpros.local:57400/blog/how-high-does-wind-speed-need-to-be-to-damage-a-home/>

- Allaire J, Xie Y, McPherson J, Luraschi J, Ushey K, Atkins A, Wickham H, Cheng J, Chang W, Iannone R (2021). *Rmarkdown: Dynamic Documents for r*. Retrieved from <https://CRAN.R-project.org/package=rmarkdown>
- Bengtsson H (2021). *R.utils: Various Programming Utilities*. Retrieved from <https://github.com/HenrikBengtsson/R.utils>
- Hadhazy A (2011, May). “How a Tornado Can Destroy a House.” *Popular Mechanics*. Retrieved from <https://www.popularmechanics.com/outdoors/survival/stories/gone-in-four-seconds-how-a-tornado-destroys-a-house>
- Kim HJ, Durbin PA (1988). “Observations of the Frequencies in a Sphere Wake and of Drag Increase by Acoustic Excitation.” *The Physics of Fluids*, **31**(11), 3260–3265. <https://doi.org/10.1063/1.8666937>.
- Sakamoto H, Haniu H (1990). “A study on vortex shedding from spheres in a uniform flow.” *ASME Journal of Fluids Engineering*, **112**, 386–392.
- Tessner T (2021, August). “What Are Hurricane Shutters? An Introduction to Hurricane Shutters.” *Eurex Shutters*. Retrieved from <https://eurexshutters.com/what-are-hurricane-shutters/>
- Urbanek S (2021). *Jpeg: Read and Write JPEG Images*. Retrieved from <http://www.rforge.net/jpeg/>
- Xie Y (2013). “animation: An R Package for Creating Animations and Demonstrating Statistical Methods.” *Journal of Statistical Software*, **53**(1), 1–27. Retrieved from <https://doi.org/10.18637/jss.v053.i01>
- Xie Y (2014). “Knitr: A Comprehensive Tool for Reproducible Research in R.” In *Implementing reproducible computational research*, eds. V Stodden, F Leisch, and RD Peng,. Chapman; Hall/CRC. Retrieved from <http://www.crcpress.com/product/isbn/9781466561595>
- Xie Y (2015). *Dynamic Documents with R and Knitr* 2nd ed. Chapman; Hall/CRC, Boca Raton, Florida. Retrieved from <https://yihui.org/knitr/>
- Xie Y (2021a). *Animation: A Gallery of Animations in Statistics and Utilities to Create Animations*. Retrieved from <https://yihui.org/animation/>
- Xie Y (2021b). *Knitr: A General-Purpose Package for Dynamic Report Generation in r*. Retrieved from <https://yihui.org/knitr/>
- Xie Y, Allaire JJ, Grolemund G (2018). *R Markdown: The Definitive Guide*. Chapman; Hall/CRC, Boca Raton, Florida. Retrieved from <https://bookdown.org/yihui/rmarkdown>
- Xie Y, Dervieux C, Riederer E (2020). *R Markdown Cookbook*. Chapman; Hall/CRC, Boca Raton, Florida. Retrieved from <https://bookdown.org/yihui/rmarkdown-cookbook>

10. Acknowledgements

Thank you so much for reading this work!

Affiliation:

Justin Campbell
Aerospace Department, University of Texas at Austin
E-mail: Campbelljustin989@gmail.com - jsc4348

Affiliation:

Amanda Hiett
Aerospace Department, University of Texas at Austin
E-mail: hiett.mandy@utexas.edu - amh7427

Affiliation:

Akhil Sadam
Aerospace Department, University of Texas at Austin
E-mail: akhil.sadam@utexas.edu - as97822